

ROLE OF ATF4 IN DIRECTING GENE EXPRESSION IN THE BASAL STATE  
AND DURING THE UNFOLDED PROTEIN RESPONSE IN LIVER

Michael Edward Fusakio

Submitted to the faculty of the University Graduate School  
in partial fulfillment of the requirements  
for the degree  
Doctor of Philosophy  
in the Department of Biochemistry and Molecular Biology,  
Indiana University

August 2016

Accepted by the Graduate Faculty, Indiana University, in partial fulfillment of the requirements for the degree of Doctor of Philosophy.

Doctoral Committee

---

Ronald C. Wek, PhD., Chair

June 13, 2016

---

Millie M. Georgiadis, PhD.

---

Yunlong Liu, PhD.

---

Howard C. Masuoka, PhD.

---

Lawrence Quilliam, PhD.

---

John J. Turchi, PhD.

© 2016

Michael Edward Fusakio

## **DEDICATION**

I would like to dedicate this accomplishment to my wife, Jennifer, who was there through all the highs and the occasional lows of graduate school.

## **ACKNOWLEDGEMENTS**

I want to acknowledge my friends, family, and coworkers for their support in all manners during my academic training and life in general. I would like to thank Dr. Peter Roach and the NIH for the support through the T32 Training Grant. I would like to thank my committee members for the countless discussions and time spent concerning my work. I thank Dr. Millie Georgiadis for her astute critical observations, which have improved my ability to think on my feet. I thank Dr. Yunlong Liu for his insight and expertise into the field of Bioinformatics. I thank Dr. Howard Masuoka for sharing his vast clinical knowledge which greatly improved the quality and impact of my work. I'd like to acknowledge Dr. Lawrence Quilliam for his commitment, time, and helpful comments. I'd like to thank Dr. John Turchi for his support, time, humor, and critiques. Finally, I would like to extend a special acknowledgment to Dr. Ronald Wek. The research environment he created emphasized quality research, and the commitment necessary to achieve that quality.

Michael Edward Fusakio

ROLE OF ATF4 IN DIRECTING GENE EXPRESSION IN THE BASAL STATE  
AND DURING THE UNFOLDED PROTEIN RESPONSE IN LIVER

Disturbances in membrane composition and protein folding in the endoplasmic reticulum (ER) trigger the unfolded protein response (UPR). Three UPR sensory proteins, PERK (PEK/EIF2AK3), IRE1, and ATF6 are each activated by ER stress. PERK phosphorylation of the alpha subunit of eIF2 represses global protein synthesis, lowering influx of nascent polypeptides into the stressed ER, coincident with the preferential translation of *ATF4* (CREB2). Results from cultured cells demonstrate that ATF4 induces transcriptional expression of genes directed by the PERK arm of the UPR, including genes involved in amino acid metabolism, resistance to oxidative stress, and the proapoptotic transcription factor CHOP (GADD153/DDIT3). In this study, we characterized two *ATF4* knockout mouse models and show in liver exposed to ER stress that ATF4 is not required for *CHOP* expression, but rather ATF6 is a primary inducer. RNA-sequence analysis indicated that ATF4 was responsible for a small portion of the PERK-dependent genes in the UPR. This smaller than expected subset of gene expression lends itself to the relevance of UPR crosstalk, with ATF6, XBP1, and CHOP being capable of upregulating UPR genes in the absence of ATF4. RNA-sequence analysis also revealed a requirement for expression of *ATF4* for expression of a comparable number of genes basally, including those involved in oxidative stress response and cholesterol metabolism. Consistent with this pattern of gene expression, loss of

*ATF4* in our mouse model resulted in enhanced oxidative damage and increased free cholesterol in liver under stress accompanied by lowered cholesterol in sera. Taken together, this study highlights both an expansion of the role of ATF4 in transcriptional regulation of genes involved in metabolism in the basal state and a more specialized role during ER stress. These findings are important for understanding the variances of the UPR signaling between cell culture and *in vivo* and for a greater understanding of all the roles ATF4 plays within the cell.

Ronald C. Wek, PhD., Chair

## TABLE OF CONTENTS

<b>LIST OF TABLES</b> .....	xi
<b>LIST OF FIGURES</b> .....	xi
<b>ABBREVIATIONS</b> .....	xiii
<b>CHAPTER 1. INTRODUCTION</b>	
1.1 Stress and the Unfolded Protein Response .....	1
1.2 PERK phosphorylation of eIF2 directs translational control .....	4
1.3 Activation of the ATF6 and IRE1 arms of the UPR .....	8
1.4 ER stress and transcriptional control .....	9
1.5 Nutrient stress and ATF4 transcriptional control.....	10
1.6 Oxidative stress and the Unfolded Protein Response .....	11
1.7 Cholesterol and lipid metabolism and the Unfolded Protein Response .....	13
1.8 ATF4 regulates gene expression during the basal state and has tissue-specific functions .....	15
1.9 The Unfolded Protein Response and Disease.....	19
1.10 Role of ATF4 in the liver during the Unfolded Protein Response .....	21
<b>CHAPTER 2. EXPERIMENTAL METHODS</b>	
2.1 Cell Culture. ....	22
2.2 Measurement of eIF2 $\alpha$ -P and UPR by immunoblot analyses.....	23
2.3 Interpreting the observed induction of eIF2 $\alpha$ -P and the UPR activation during ER stress.....	26
2.4 Animals.....	26
2.5 Reverse transcription and real-time PCR.....	27



2.6	Histology .....	29
2.7	Cholesterol measurements.....	29
2.8	RNA-Seq analysis.....	30
2.9	PANTHER Overrepresentation Test.....	31
2.10	Generation of Volcano Plots .....	31
2.11	Lipid Peroxidation measurements .....	32
2.12	Mitochondrial Membrane Potential Measurements .....	33
2.13	Luciferase Assays.....	33
2.14	Cell Survival Assays .....	35
2.15	Statistics .....	36

**CHAPTER 3. RESULTS: ATF4 IS REQUIRED FOR A PARTICULAR  
SUBSET OF UNFOLDED PROTEIN RESPONSE GENES**

3.1	UPR signaling differs between cell culture models.....	37
3.2	Liver cell culture requires ATF6 for optimal <i>CHOP</i> expression. ....	42
3.3	ATF4 and ATF6 both drive <i>CHOP</i> expression during nutritional stress. ....	46
3.4	Comparison of ATF4 and ATF4/ <i>CHOP</i> target genes in <i>ATF4</i> knockout mouse. ....	50
3.5	Loss of <i>ATF4</i> in a mouse model mimics cell culture model increase in oxidative stress but shows minimal cellular death.....	56
3.6	RNA-Seq Analysis of liver-specific <i>ATF4</i> knockout mice demonstrates a particular subset for ATF4 transcriptional responsibilities. ....	56
3.7	<i>ATF4</i> facilitates the metabolism of cholesterol in the liver. ....	62

3.8 ATF4 basal expression is required for lipid metabolism ..... 66

**CHAPTER 4. DISCUSSION**

4.1 Similarities and differences in UPR signaling between  
cell culture models. .... 68

4.2 The role of crosstalk in the UPR..... 69

4.3 Role of ATF4 in the ER stress response *in vivo*..... 72

4.4 ATF4 and cholesterol metabolism..... 73

4.5 Role of ATF4 in gene expression during basal state..... 75

**REFERENCES** ..... 77

**Curriculum vitae**

## LIST OF TABLES

Table 2-1	Sequence of primers for SYBR green based qRT-PCR.....	28
Table 2-2	Code for generation of volcano plots.....	32
Table 2-3	Plasmids used in this study.....	34
Table 3-1	Pathway analysis using PANTHER of altered genes in WT and LsATF4-KO livers during non-stressed conditions. ....	59
Table 3-2	Pathway analysis using PANTHER of regulated genes in WT and LsATF4-KO livers during treatment with tunicamycin.....	60
Table 3-3	Comparison of altered gene expression in the absence of ATF4 in basal and stress states with genes bound by ATF4 or ATF4 and CHOP.....	60

## LIST OF FIGURES

Figure 1-1	The Unfolded Protein Response.....	3
Figure 1-2	Control of the expression of <i>ATF4</i> occurs at multiple steps.....	7
Figure 1-3	<i>ATF4</i> and its role in Physiology .....	16
Figure 3-1	Hepa1-6 cells demonstrate an <i>ATF4</i> -independent <i>CHOP</i> expression. ....	40
Figure 3-2	<i>ATF6</i> facilitates induced <i>CHOP</i> expression in liver cells subjected to ER stress.....	44
Figure 3-3	<i>ATF6</i> contributes to <i>CHOP</i> expression in multiple stresses .....	48
Figure 3-4	<i>CHOP</i> expressed independent of <i>ATF4</i> in whole-body <i>ATF4</i> knockout livers. ....	52
Figure 3-5	<i>CHOP</i> is expressed independent of <i>ATF4</i> in liver-specific <i>ATF4</i> knockout mice.....	54
Figure 3-6	<i>ATF4</i> is required for expression of a subset of UPR genes.....	61
Figure 3-7	Loss of <i>ATF4</i> leads to increased free cholesterol in liver .....	64
Figure 3-8	Loss of <i>ATF4</i> leads to reduced expression of <i>CRLS1</i> .....	67

## ABBREVIATIONS

AARE	Amino Acid Response Element
ASNS	Asparagine Synthetase
ATF3	Activating Transcription Factor-3
ATF4	Activating Transcription Factor-4
ATF5	Activating Transcription Factor-5
ATF6	Activating Transcription Factor-6
ATF6(N)	Activating Transcription Factor-6 N-terminus
bZIP	Basic Leucine Zipper
CARE	CCAAT-enhancer binding protein Activating Transcription Factor (C/EBP-ATF) Response Element
CHOP	C/EBP Homologous Protein
CTH	Cystathionine gamma-lyase
DMEM	Dulbecco's Modified Eagle's Media
eIF2	Eukaryotic Initiation Factor 2
eIF2 $\alpha$	Eukaryotic Initiation Factor-2 $\alpha$
eIF2 $\alpha$ -P	Eukaryotic Initiation Factor-2 Phosphorylation
ER	Endoplasmic Reticulum
ERSE	Endoplasmic Reticulum Stress Response Element
FGF21	Fibroblast Growth Factor 21
GAP	GTPase-Activating Protein
GDP	Guanosine Diphosphate
GTP	Guanosine-5'-Triphosphate
GADD34	Growth Arrest and DNA Damage-inducible protein-34

HMG-CoA	3-hydroxy-3-methylglutaryl coenzyme A
IP	Intraperitoneal
ISR	Integrated Stress Response
IRE1	Inositol Requiring Enzyme -1
LsATF4-KO	Liver-Specific ATF4 Knockout Mouse
LsPERK-KO	Liver-Specific PERK Knockout Mouse
MDA	Malondialdehyde
Met-tRNA <sub>i</sub>	Methionyl-Initiator tRNA
MEF	Mouse Embryonic Fibroblast
NASH	Nonalcoholic steatohepatitis
NT	No treatment
PCR	Polymerase Chain Reaction
PEK	Pancreatic eIF2 kinase
PERK	PKR-Like ER kinase
RIP	Regulated Intramembrane Proteolysis
ROS	Reactive Oxygen Species
SREBP	Sterol regulatory element-binding protein
qPCR	Quantitative PCR
UPR	Unfolded Protein Response
UTR	Untranslated Region
uORF	upstream Open Reading Frame
WbATF4-KO	Whole Body ATF4 Knockout Mouse
WT	wild-type

WRS	Wolcott-Rallison Syndrome
XBP1	X-Box Binding Protein 1

## CHAPTER 1. INTRODUCTION

### 1.1 Stress and the Unfolded Protein Response

The endoplasmic reticulum (ER) is a central hub for protein and lipid metabolism, and disruptions in ER homeostasis can trigger the Unfolded Protein Response (UPR). The UPR features transcriptional and translational control mechanisms that collectively serve to enhance protein folding and assembly, thereby expanding the capacity of the ER to process proteins slated for the secretory pathway [1-3]. Additionally, the ER is instrumental for intermediary and complex lipid metabolism [4]. Among lipids, prudent regulation of cholesterol synthesis is critical as cholesterol helps to order phospholipids in membranes. UPR sensory proteins, such as the Type 1 ER transmembrane protein kinase PERK (EIF2AK3/PEK), are activated by disruptions in protein folding or membrane compositions. The ensuing PERK phosphorylation of the  $\alpha$  subunit of eIF2 (eIF2 $\alpha$ -P) represses global protein synthesis, thereby reducing the influx of nascent polypeptides into the overloaded ER. Coincident with global translational control, eIF2 $\alpha$ -P enhances preferential translation of a subset of stress-related mRNAs, including *ATF4* (*CREB2*), a transcriptional activator of UPR target genes [5-7]. Because eIF2 $\alpha$ -P induces *ATF4* translational expression in response to a range of environmental and physiological stresses, in addition to those afflicting the ER, the ATF4-directed regulatory scheme has been referred to as the Integrated Stress Response (ISR) [2, 6].

Activation of PERK during ER stress is accompanied by induction of the additional arms of the UPR that feature ER transmembrane proteins ATF6 and



IRE1 (Figure 1-1) [1, 8]. Activation of the IRE1 and ATF6 pathways elicit multiple downstream effects to limit the strain of proteotoxicity on the cell. IRE1 is a protein kinase and riboendonuclease that serves to facilitate the cytosolic splicing of XBP1 mRNA, leading to translation of an activated version of the transcription factor, XBP1s, that induces UPR genes involved in protein folding, degradation of unfolded or misfolded proteins, and membrane expansion and renewal [9-16]. The endoribonuclease activity of IRE1 also cleaves mRNAs in the proximity of the ER, so-called regulated IRE1-dependent decay (RIDD), which changes the composition of mRNAs available for translation [17, 18]. In response to ER stress, ATF6 induces transcriptional expression of chaperone proteins necessary for assisting in the folding of unfolded proteins and leads to increases in the expansion of the ER, increasing its capacity [19, 20].

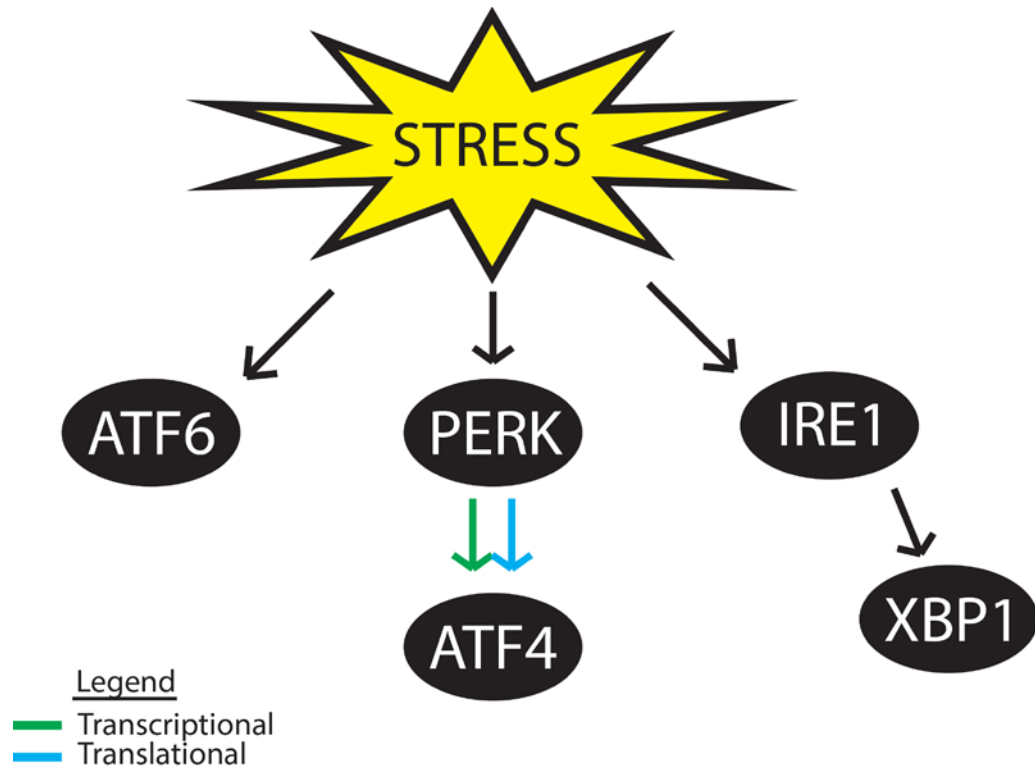


**Figure 1-1 The Unfolded Protein Response.** ER stress leads to the activation of the unfolded protein response. PERK activation leads to the phosphorylation of eIF2 $\alpha$  and the transcriptional and translational upregulation of ATF4. IRE1 activation results in the splicing of *XBP1* mRNA, resulting in the active transcription factor XBP1s. Finally, ATF6 is translocated to the Golgi where it undergoes a cleavage event releasing the active transcription factor.

The UPR sensors PERK, ATF6, and IRE1 pathways are often viewed as functioning in parallel and, with branch of the UPR having the potential to elicit different effects on cell viability [1, 21, 22]. For example, PERK is posited to promote cell death by enhancing *CHOP* expression, whereas IRE1 is suggested to support cell survival during ER stress [21, 23, 24]. Mice with whole body knockouts for ATF6 showed delayed recovery from ER stress and decreased survival [21]. The premise of distinct sensory pathways in the UPR is challenged by the emerging findings that there is cross-regulation between the UPR branches. This idea is illustrated by the report that loss of *PERK* in cultured cells or livers of mice, or deletion of *ATF4* in cultured mouse embryonic fibroblast (MEF) cells, substantially ablated activation of ATF6 and reduced expression of XBP1s during ER stress [25]. Crosstalk in the UPR can also regulate PERK, with for example XBP1s inducing transcriptional expression of p58<sup>IPK</sup>, which is reported to lower PERK phosphorylation of eIF2 $\alpha$  and translational control [11, 26]. Therefore, it is likely that the UPR represents an interconnected network of regulatory proteins that function together to modulate gene expression that helps restore protein homeostasis during the progression of the UPR [27].

## **1.2 PERK phosphorylation of eIF2 directs translational control**

The global repression of translation caused by the phosphorylation of the  $\alpha$  subunit of eIF2 reduces the incoming translational load on the ER [8, 28]. This repression is a result of eIF2 being a part of the translation preinitiation complex, consisting of 40S ribosomes associated with eIF2 bound with GTP and Met-

tRNA<sup>Met</sup>. The preinitiation complex binds at the 5'- "cap" complex of the mRNA and then scans the mRNA processively 5' to 3' until it reaches the initiation codon. Prior to reaching the initiation codon, GTP is hydrolyzed to GDP with the help of the GAP eIF5, allowing for the joining of the 60S ribosome and formation of the 80S ribosome [29]. The eIF2-GDP is released from the translational machinery, and the GDP on eIF2 must be exchanged for GTP prior to the next round of translation initiation. This eIF2 exchange occurs through the guanine nucleotide exchange factor, eIF2B. eIF2B is inhibited by eIF2 $\alpha$ -P, preventing the eIF2-GDP to GTP conversion. eIF2-GDP is unable to complex with Met-tRNA<sup>Met</sup>, preventing the formation of the 43S complex. Reduced levels of the 43S ribosomal complex blocks ribosome loading onto mRNAs and subsequent scanning, and as a consequence there are sharp reductions in translation that conserve energy during stress conditions [2].

Coincident with repression of global protein synthesis, PERK phosphorylation of eIF2 $\alpha$  leads to preferential translational of select mRNAs, the most well-known target being *ATF4* [7]. The 5'-leader of *ATF4* mRNA contains two upstream open reading frames (uORFs) with the second of these two elements overlapping out-of-frame with the *ATF4* coding sequence (Figure 1-2). During periods of non-stress, ribosomes translate the first 5'-proximal open reading frame, uORF1, and then due to the higher levels of eIF2-GTP are able to rapidly reinitiate at the next ORF, uORF2. Reinitiation of translation at uORF2, which overlaps out-of-frame with the *ATF4* coding sequence, prevents synthesis of *ATF4* protein. In stress conditions, ribosomes translate uORF1 and resume

scanning along the 5'-leader of the ATF4 mRNA. However, with eIF2 $\alpha$  phosphorylation there are low eIF2-GTP levels that significantly delay the scanning ribosome from reacquiring eIF2-GTP coupled with Met-tRNA<sup>Met</sup>. As a result the ribosome reinitiates at the *ATF4* coding sequence culminating in increased ATF4 protein. Levels of ATF4 protein can also be altered by post-translational modifications, including phosphorylation, which can allow for interaction with SCF <sup>$\beta$ TrCP</sup> that leads to the ubiquitination and degradation of ATF4 by proteasomes [30]. Elevated ATF4 expression and expression of its heterodimerization partners directly contributes to increased transcription of its targeted genes.

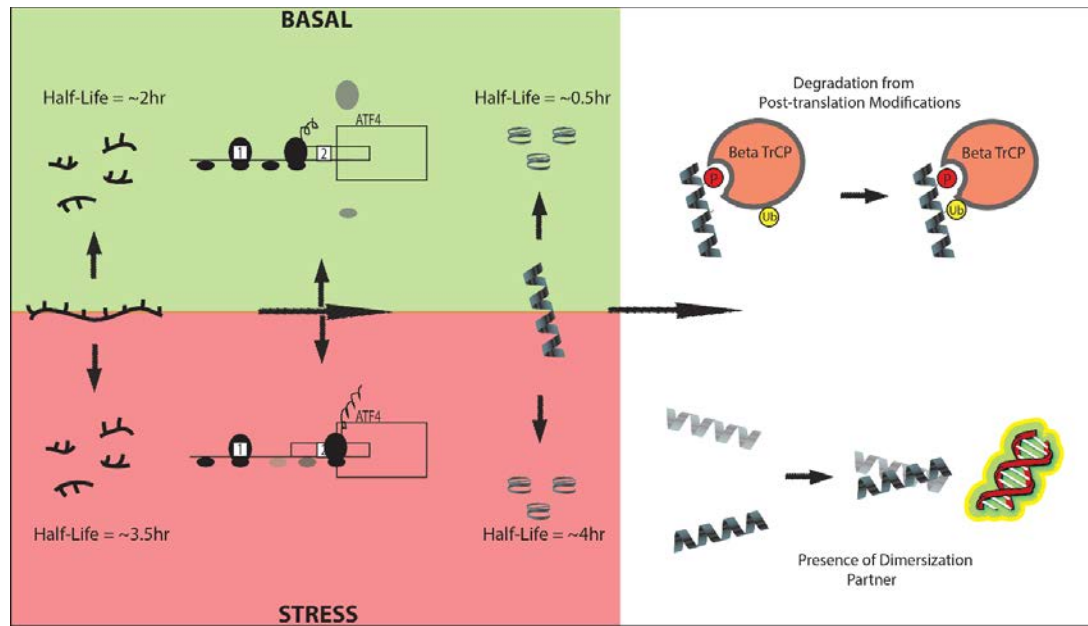


**Figure 1-2 Control of the expression of *ATF4* occurs at multiple steps.**

Control of *ATF4* expression occurs at multiple steps involving both the synthesis and decay of mRNA and protein. During a stress event, the half-life of *ATF4* mRNA and protein are increased, leading to increased levels of *ATF4* mRNA [31]. This increase in stability is accompanied by the translational upregulation due to the delayed reinitiation. *ATF4* can undergo post-translational modifications, including phosphorylation, which can allow interaction with the SCF<sup>βTrCP</sup> leading to the ubiquitination and degradation of *ATF4* [30]. *ATF4* transcriptional activity can also be controlled through the presence of its heterodimerization partners.

### 1.3 Activation of the ATF6 and IRE1 arms of the UPR

In addition to PERK, two other UPR sensors, ATF6 and IRE1, function to regulate transcriptional expression. Upon ER stress, the accumulation of

misfolded proteins is suggested to inhibit the interaction between ATF6 and BiP. The full-length membrane-bound transcription factor ATF6 is then trafficked from the ER to the Golgi by COPII vesicles [32, 33]. In the Golgi, ATF6 undergoes regulated intramembrane proteolysis (RIP) via site 1 (S1P) and site 2 proteases (S2P), releasing the N-terminal ATF6 segment, ATF6(N) [21, 32, 34-37].

ATF6(N) then traffics to the nucleus where it induces gene expression associated with several downstream functions of the UPR including upregulation of the protein chaperone, such as *BiP*, to assist in proper folding, expansion of the ER, and upregulation of expression of *XBP1* [15, 19, 20, 38]. Mutations in ATF6, have been associated with photoreceptor degeneration and achromatopsia [39, 40], conditions which are associated with reduced visual acuity or blurriness and sensitivity to light.

During ER stress, IRE1 undergoes oligomerization and transautophosphorylation, which are also hallmark features of PERK activation [41]. These events lead to the activation of IRE1 endoribonuclease activity. As described earlier, IRE1 initiates the cytosolic splicing of *XBP1* mRNA, which removes a 26 nucleotide segment from the *XBP1<sub>u</sub>* mRNA. This cleavage event and the subsequent ligation of XBP1 by the catalytic subunit of the tRNA ligase complex result in a translation frame shift, which removes a stop codon allowing for translation of active XBP1s [42].

#### **1.4 ER stress and transcriptional control**

ATF4 serves to enhance transcriptional expression of genes involved in amino acid metabolism and resistance to oxidative stress [6, 43-45]. ATF4 also upregulates the transcription of many of the genes involved in amino acid synthesis [6, 46]. Most notable is the transcription of the gene *ASNS*, encoding asparagine synthetase, which catalyzes the conversion of aspartate to asparagine [43]. Activation of the *ASNS* gene occurs at a promoter element known as an Amino Acid Response Element (AARE) [47]. ATF4 binding at the AARE element, as with many of its target genes, requires ATF4 heterodimerization with other basic zipper proteins, such as C/EBP $\beta$ . Binding of ATF4 heterodimers at the AARE elements in target gene promoters can result in histone acetylation, which leads to the recruitment of general transcription machinery including RNA polymerase II, leading to induced gene transcription [48]. During prolonged periods of stress, ATF4 heterodimerization and binding at AAREs can be disrupted by increased expression of ATF3. ATF3 can compete with ATF4 for interaction with C/EBP $\beta$ , thereby decreasing ATF4 binding at target promoters, such as *ASNS*, which lowers gene expression. Thus, there is a dynamic process of ATF4-directed gene expression during the progression of a stress response, with an early full induction of target genes, followed by a dampening of expression as a network of transcription factors is expressed and differentially engages with the promoters of stress responsive genes.

ATF4 has a major role in prevention of oxidative stress. This is illustrated by the finding that ATF4 depletion in MEF cells, even in the absence of apparent stress sharply increases oxidative stress as measured by a reduction in cell



death upon the addition of antioxidant [6]. As a consequence, *ATF4*<sup>-/-</sup> MEF cells demonstrated lowered survival unless the medium was supplemented with reducing agents, such as cysteine or  $\beta$ -mercaptoethanol. Cysteine is a major component of the synthesis of glutathione, a reductant in the cell [49], and ATF4 was found to be important for expression of *CTH* (or *CSE*), a gene responsible for converting cysteine from cystathionine, for the purpose of generating glutathione [46].

ATF4 also functions to induce expression of another transcription factor, CHOP, and ATF4 and CHOP independently or in combination are thought to coordinate key facets of the UPR transcriptional and translational control directed by PERK [6, 50-55]. For example, together ATF4 and CHOP induce the expression of *GADD34*, which serves to direct feedback dephosphorylation of eIF2 $\alpha$ -P [55-59]. ATF4 and CHOP also function in a feedforward loop to induce expression of a related transcription factor ATF5, and this transcription network is central for determining cell fate in response to ER stress [51].

### **1.5 Nutrient stress and ATF4 transcriptional control**

Mammalian cells sense amino acid availability via two mechanisms, the first being the mTORC1 pathway which functions to maintain a necessary quantity of amino acids to maintain the current protein rate of synthesis and cell growth [60, 61]. mTORC1 activation during periods of high amino acid content occurs at the surface of late endosomes and lysosome via Rag complexes [62]. High levels of amino acids cause Ragulator to activate RagA, resulting in the

formation of active RagA/RagC complex, which recruits mTORC1 to the lysosome and allows its interaction with Rheb, which activates mTORC1 [62, 63]. Deficiency for essential amino acids also triggers the amino acid response pathway. This pathway features activation of GCN2, which phosphorylates eIF2 $\alpha$  and triggers repression of general translation, which serves to conserve consumption of amino acids [2, 61]. Coincident with the regulation of global protein synthesis, eIF2 $\alpha$ -P selectively enhances expression of certain genes that serve to restore the levels of the depleted amino acid. ATF4, which as noted earlier is preferentially translated during periods of eIF2 $\alpha$  phosphorylation, is a central regulator of genes involved in nutrient uptake and metabolism, including ASNS and the amino acid transporter *SLC7a11*, and genes that participate in protein degradation, which collectively serve to increase the pool of available amino acids [2]. ATF4 also induces expression of Sestrin2, which regulates Rag GAP complex GATOR [64, 65]. The ATF4 connection to mTORC1 is also present in hypoxic stress through ATF4 induction of REDD1, which also inhibits mTORC1 signaling [66]. This stress response results in similar outcomes to the PERK driven stress response, with GADD34 driven dephosphorylation of eIF2 $\alpha$  leading to a restoration of general synthesis or in cases of prolonged stress, cell death.

## **1.6 Oxidative stress and the Unfolded Protein Response**

Reactive oxygen species at appropriate concentrations play a beneficial role and allow for certain necessary reactions to occur in cells. These beneficial

effects include energy production through oxidative phosphorylation, cellular growth, and degradation via the peroxisomes [67, 68]. When levels of ROS exceed the antioxidant defense of cells, ROS instead results in lipid peroxidation and damage to DNA [68]. ROS can be generated by several organelles in the cell, with the mitochondria and the ER being two of the major sources of ROS. ROS generation in the ER occurs as a result of the ER environment promoting protein disulfide bond formation via the protein disulfide isomerase family. Glutathione in the ER acts to reduce disulfide bonds, generating oxidized glutathione, which is at much higher levels in the ER than other compartments of the cell [68]. However, ROS production in the mitochondria results as a by-product of energy production from the electron transport chain.

*PERK*<sup>-/-</sup> cells have been shown to accumulate endogenous peroxides during ER stress, demonstrating the important role of the UPR in alleviating oxidative damage [6]. However, *PERK*-deficient cells did not show accumulation of peroxides in basal conditions or need reducing agent supplementation in the medium. By comparison, *ATF4*<sup>-/-</sup> MEF cells failed to thrive in basal conditions without supplementation of the media with an antioxidant [6]. Genome-wide mRNA analysis via microarray of cells depleted for ATF4 indicated that this transcription factor is critical for expression of genes involved in the metabolism of sulfur-containing amino acids, which is likely one important reason for the antioxidant functions of ATF4 [6].

## 1.7 Cholesterol and Lipid Metabolism and the Unfolded Protein Response

The liver plays a major role in the processing of lipids, and the ER serves as the major locus for lipid metabolism within the liver [69]. Fatty acids are generated from the hydrolysis of triglycerides in lipid droplets, uptake from the circulation, or via *de novo* synthesis. Lipid levels are controlled primarily through the sterol regulatory element-binding protein (SREBP) family of transcription factors. SREBP1c is necessary for the *de novo* lipid synthesis, whereas SREBP2 regulates cholesterol metabolism [70]. Like ATF6, the SREBPs are transcription factors activated by regulated intramembrane proteolysis (RIP) and are released from the ER membrane through an interaction with the proteins SCAP and INSIG [37]. Dissociation of SREBP/SCAP from INSIG due to low sterol levels results in SREBP transport to the Golgi. Once in the Golgi, SREBP undergoes a cleavage event by the same proteases that cleave ATF6, S1P and S2P [71]. SREBPs are then translocated to the nucleus where they activate genes involved in lipid and cholesterol metabolism. ER stress has been shown to increase the proteolytic cleavage of SREBPs by degradation of INSIG [69]. However, ER stress elicited by tunicamycin represses transcription of SREBP1 [70].

Cholesterol levels within the liver are maintained via multiple pathways involving synthesis, export, and import via particular transporters, esterification, and conversion into bile acids. Approximately 10-20% of cholesterol synthesis occurs within the liver and originates with the conversion of three molecules of acetate into 3-hydroxy-3-methylglutaryl coenzyme A (HMG-CoA) [72, 73]. HMG-

CoA is then converted to mevalonic acid by HMG-CoA reductase, and after several additional biochemical steps forms cholesterol. HMG-CoA reductase is the rate-limiting step and can be inhibited by high levels of cholesterol in a negative feedback loop. Cholesterol cannot be broken down into carbon and water and thus must be removed through conversion or excretion. Of the cholesterol that enters the intestinal system, 50% will be reabsorbed, with the remainder being excreted via the stool. HMG-CoA reductase levels are upregulated by SREBP2, whose activation is controlled in a manner similar to SREBP1 [73]. Whereas SREBP2 levels do not appear to be reduced in response to stress, expression of HMG-CoA reductase is lowered in the liver [25]. Dysfunction in the cholesterol biosynthetic pathway is believed to play a role in the development and/or progression of non-alcoholic fatty liver disease and non-alcoholic steatohepatitis (NASH). Patients with non-alcoholic fatty liver disease demonstrate increased expression of active SREBP2 and HMG-CoA, which correlate to increased free cholesterol levels [73]. Tight regulation of cholesterol synthesis is required to ensure a balance between maintaining membrane integrity and proper cellular metabolism and preventing accumulation of potentially damaging cholesterol.

Previous studies have suggested that PERK plays a role in lipid homeostasis. Liver-specific PERK knockout (LsPERK-KO) mice showed increased levels of Oil Red O after 12-hour tunicamycin treatment, signifying an increase in fat deposits [25]. Livers from LsPERK-KO mice also displayed increased levels of triglycerides after 12 hours of the tunicamycin treatment.

*SREBP1* expression was reduced in WT and LsPERK-KO mice in response to stress, despite the accumulation of lipids, suggesting that accumulation of lipids results from a failure to excrete or metabolize lipids rather than an increase in lipid synthesis.

### **1.8 ATF4 regulates gene expression during the basal state and has tissue-specific functions**

Expression of *ATF4* is typically viewed in the context of stress responses, where ATF4 levels can be increased in multiple tissue types including liver, pancreas, brain, and brown and white adipose tissues [74]. Yet, there is growing evidence that ATF4 has a role that pertains to the development of different tissue types (Figure 1-3), as well as a role in mitochondrial functions.

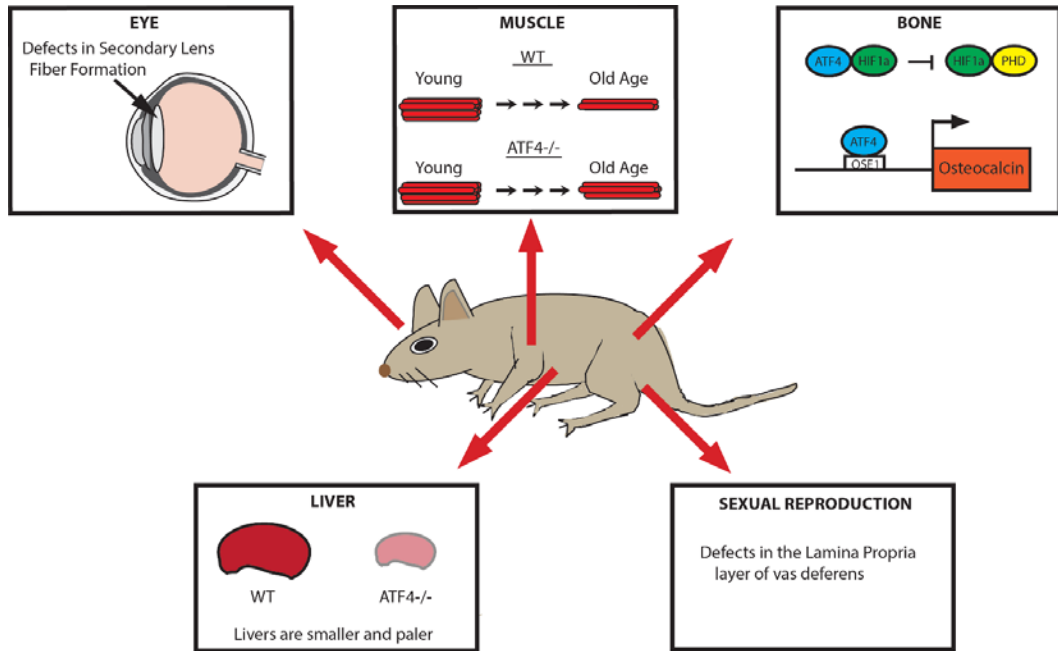


**Figure 1-3. ATF4 and its Role in Physiology.** Loss of ATF4 has been associated with several physiological alterations. *ATF4* knockout mice demonstrate a failure of certain cells to differentiate in their eyes, bones, and reproductive organs [75-77]. The *ATF4*<sup>-/-</sup> mice also show anemia in the fetal liver, and lack of angiogenesis in the bone [78]. *ATF4*<sup>-/-</sup> mice also present with resistance to muscle weakening due to fasting or old age [79, 80].

*ATF4* knockout mice are born with severe microphthalmia and absent lens [77]. Eye lens development results from two differentiation processes. The primary lens differentiation in *ATF4*<sup>-/-</sup> mice occurs normally, with primary lens fiber cells showing no significant difference between wild-type (WT) and *ATF4*<sup>-/-</sup> mice at E14.5 [77]. Differentiation of secondary lens fiber cells results from the proliferation of lens epithelial cells and subsequent conversion of these cells into secondary fiber cells. Loss of *ATF4* did not lead to alteration in the proliferation of epithelial cells but did impede differentiation of secondary lens fiber cells, resulting in the failure to generate a lens [77].

*ATF4* is also suggested to impede differentiation of other tissues and may help explain the infertility issues commonly associated with the *ATF4*<sup>-/-</sup> mice [78]. The morphology of sperm from *ATF4*<sup>-/-</sup> and WT mice were found to be similar and capable of causing *in vitro* fertilization of WT embryos [75]. However, examination of the vas deferens from *ATF4*-deficient mice led to the discovery that there were alterations in the thickness of the tissues layers, and the lumen layer was reduced in diameter. The morphological differences in *ATF4*<sup>-/-</sup> mice were suggested to result from failure of elastin in the lamina propria to polymerize into elastic fibers during sexual maturation [75]. These developmental changes were seen at 10 weeks of age, while the mice appeared morphologically similar to WT at 5 weeks of age, prior to sexual maturation.

One of the most notable phenotypes observed in *ATF4*<sup>-/-</sup> mice occurs in bone. *ATF4*-deficient mice demonstrated reduced area of mineralized tissue within the frontal and parietal bones, along with the clavicle and long bones [76].



This delay in mineralization was also seen within the skull of the *ATF4*-deleted mice. Similar to what was seen in eye development, early skeletogenesis was unaffected by the loss of *ATF4*, with day E13 WT and *ATF4*<sup>-/-</sup> mice displaying no differences [76]. However, at E16, there was a noticeable difference in osteoblast differentiation. The osteoblast phenotype was attributed to an important role of ATF4 in expressing target genes involved in osteogenesis, such as osteocalcin [76]. Expression of osteocalcin is dependent upon ATF4 interaction with the OSE1 element in the promoter of the osteocalcin gene [81]. ATF4 binds first to the OSE1 element and then interacts with the general transcription factor TFIIA $\gamma$ , which also engages with Runx2 and drives osteocalcin expression. These gene expression changes culminate in a significant reduction in bone mass in *ATF4*<sup>-/-</sup> mice [76]. Intriguingly, not all of the effects of ATF4 on bone development are thought to be anabolic. There is also evidence that ATF4 has a catabolic role in bone formation by controlling the differentiation of osteoclast. Histological sections of *ATF4*<sup>-/-</sup> mice showed reduced levels of the osteoclast enzyme tartrate-resistant acid phosphatase and lowered levels of NFATc1, the master regulator of osteoclast differentiation [82]. ATF4 was shown to bind to the promoter region of the NFATc1 gene in osteoclast-like cells upon RANKL induction, suggesting a direct role of ATF4 in driving the differentiation of osteoclasts, and its loss leads to a severe deficiency in osteoclast differentiation.

Catabolic functions of ATF4 are also seen in the muscle, where ATF4 has been associated with muscle weakness and atrophy [79, 80, 83]. During fasting

conditions it was shown that depletion of *ATF4* expression in muscle prevented the decrease seen in fiber diameter following fasting [79]. In the absence of fasting, the fiber diameter was also reduced upon overexpression of *ATF4*. This reduction in fiber density may result from lowered expression of five *ATF4*-target genes, *CDKN1A*, *CSR3*, *PEG3*, *GADD45A*, and *ANKRD1* [79]. A role for *ATF4* in the induction of muscle atrophy was also seen in response to limb immobilization [83]. *ATF4* is also suggested to play a role in the loss of muscle due to aging. Ursolic acid and tomatidine were determined to reduce age-related decreases in muscle strength and mass by a mechanism suggested to involve depletion of *ATF4* expression and activity [80]. The precise drug targets for lowered expression of *ATF4* are currently unclear, but repression of *ATF4* transcriptional expression was reported during UV stress through the C/EBP $\beta$  Lip isoform binding to the promoter region of *ATF4* and preventing its transcription, and *ATF4* mRNA is subject to decay by nonsense-mediated RNA decay [5, 84, 85].

### **1.9 The Unfolded Protein Response and Disease**

The UPR is suggested to trigger either cell survival or cell death depending on the nature and duration of the underlying stress [24, 54]. Furthermore in certain diseases, the UPR is unable to properly function due to genetic mutations that can lead to failure of segments of the UPR network to properly remedy stress. Wolcott-Rallison syndrome is a rare disease in patients with truncations or missense mutations in *PERK* [86]. This syndrome presents

with neonatal or early onset diabetes, as well as hepatic and renal complications, lowered bone mineral density, and developmental delay including mental retardation [86]. Patients with loss of PERK function die early in childhood.

Mutations have also been found in other UPR members. As noted earlier, patients with ATF6 deficiencies have eye disorders, with achromatopsia or retinitis pigmentosa [39, 40]. Achromatopsia involves defects in color perception and acuity in high light, along with blurred vision in normal light exposure [40]. Retinitis pigmentosa is a type of photoreceptor neurodegeneration of the rod photoreceptor cells in the eye, which will eventually result in loss of cone cells of the eye [39]. This results in a progressive loss of vision by the individual. While a range of phenotypes is associated with *ATF4*-deficient mice, there are currently no known human diseases originating from mutations in *ATF4*.

The UPR is also thought to play a role in progressive diseases, such as cancer and fatty liver disease. ATF4 is suggested to be an integral part of the epithelial to mesenchymal transition, which is required for metastasis of certain tumors [87]. Once detached, cells must resist cell death resulting from the loss of attachment, also called anoikis. Recent studies have shown that ATF4 promotes resistance to anoikis by upregulating autophagic and antioxidant responses [88]. The UPR has also been linked to inflammation, which occurs in the pathogenesis of NASH. Prolonged activation of the UPR resulting in *CHOP* expression, an ATF4-target gene, triggers activation of the pro-inflammatory NF- $\kappa$ B [89]. NF- $\kappa$ B then induces the expression and secretion of cytokines, leading to cell death and inflammation in the surrounding tissue. Recent studies have also noted that free

cholesterol accumulation in liver tissues correlates with the severity of the NASH [73]. Collectively, increased cholesterol levels, inflammation, and cell death are suggested to contribute to the progression towards fibrosis often observed in NASH patients.

### **1.10 Role of ATF4 in the liver during the Unfolded Protein Response**

The results in Chapter 3 of this thesis focus on the central role of ATF4 in controlling transcriptional expression directed by PERK. In order to determine the functional roles of ATF4 in the UPR, we measured the UPR transcriptome in mice deleted for *ATF4* in the liver and compared those changes with gene expression patterns altered by depletion of *ATF4* in cultured cells. While expression of *ATF4* is induced in response to stress and the transcription factor plays a role in stress adaptation, a similar number of genes show ATF4-dependence for mRNA expression in basal conditions, with no apparent stress. ATF4 plays a role in these conditions in anti-oxidation and in cholesterol metabolism. Importantly, we also showed that ATF4 was required for only a subset of PERK-dependent genes *in vivo*. Distinct from loss of *PERK* in liver, we found that deletion of *ATF4* in liver was not required for induction of either UPR transcription factors CHOP or ATF6 during ER stress. Furthermore, deletion of ATF4 showed a ten-fold increase in hepatocyte cell death in response to ER stress. Although significant, the level of cell death resulting from deletion of ATF4 in liver was only a fraction of the cell death determined for *PERK* deficiency.

## CHAPTER 2. EXPERIMENTAL METHODS

This section will describe the techniques used in experiments and analysis described in this thesis. These experimental methods will also note points of interest and experimental considerations when studying the UPR.

### 2.1 Cell Culture

WT and *ATF4*<sup>-/-</sup> MEF cells [6], mouse hepatoma Hepa1-6 cells and HEK293T were cultured in DMEM (4.5 g/l glucose) supplemented with 1x nonessential amino acids (HyClone SH3023.01), 1x MEM essential amino acids (HyClone SH30598.01), and 50  $\mu$ M  $\beta$ -mercaptoethanol, as described previously [6]. Cultured cells were treated with solvent alone referred to as no treatment (NT), 2  $\mu$ M tunicamycin (Tm), 1  $\mu$ M MG132, or 50 nM halofuginone (HF), for the indicated times. Cultured cells that were treated with halofuginone were first washed with PBS to remove DMEM media to ensure the removal of amino acids, prior to addition of media containing dialyzed FBS and subsequent addition of halofuginone. The timing and concentration of the drug are important for each UPR experiment. Induction of UPR mRNA expression can occur as early as 3 hours making it a good initial time point. At 6 hours most members of the UPR can be detected via immunoblot analyses. Apoptotic markers are detectable starting between 12 to 24 hours of pharmacological induction of ER stress.

shRNA-directed knockdowns of *ATF4*, *ATF5*, *ATF6*, and *CHOP*, were performed using a lentivirus delivery system featuring Addgene third-generation plasmids and mission shRNA clones (Sigma-Aldrich, St. Louis, MO) for generation of the viral particles. The shRNAs used in this study are as follows:

*ATF4*: TRCN0000071726, TRCN0000071727, *ATF5*: TRCN0000075556, TRCN0000075553, *ATF6*: TRCN0000321326, TRCN0000321328, *CHOP*: TRCN0000103709, TRCN0000305677, and control Ctrl: TRC2-puro SHC201V. Plasmids WB984, WB985, and WB986 encoding the viral packaging and envelope components, along with the particular shRNA plasmid were co-transfected into HEK293T cells using the transfection reagent Fugene 6. On day 2 the media was replaced with a media containing 25mM HEPES buffer. Media was collected on days 3 and 4. This media was then added to the Hepa1-6 cells for 8 hours prior to at least 12 hours of recovery in normal DMEM media. The selection was performed using puromycin (10 µg/ml) and occurred until a non-transfected plate was devoid of cells. The shRNA Hepa1-6 cell lines were then expanded and examined for knockdown level.

## **2.2 Measurement of eIF2 $\alpha$ -P and the UPR by immunoblot analyses**

Cellular lysates were prepared from cultured MEF cells and Hepa1-6 cells using RIPA-buffered solution containing 50 mM Tris-HCL (pH 7.5), 150 mM sodium chloride, 1% Nonidet P-40, 0.1% SDS, 100 mM sodium fluoride, 17.5 mM  $\beta$ -glycerophosphate, 0.5% sodium deoxycholate, and 10% glycerol, that was supplemented with EDTA-free protease inhibitor cocktail (Roche, Basel, Switzerland). Protein concentrations were determined by the Lowry assay with the Bio-Rad DC protein quantification kit according to manufacturer's instructions (Bio-Rad, Hercules, CA cat no: 500-0113 and 500-0114). Equal concentrations of protein from each sample were prepared in 2x SDS sample buffer and heated

at 95°C for 5 minutes. Precision Plus Protein All Blue Prestained Protein Standard (Bio-Rad, Hercules, CA cat no: 1610373) was added to the SDS polyacrylamide gel to determine molecular weights. SDS gels were made at either 12% acrylamide or a gradient gel of 4-20% (Novus Biologicals, Littleton, CO cat no: NBP1-78903). Gel electrophoresis was then followed by transfer of proteins to nitrocellulose membranes. Membrane blots were incubated for 1 hour in 5% (w/v) nonfat milk powder in PBS with 0.2% Tween-20. Primary antibody in 5% nonfat milk powder was added to the blot overnight, and blots were then washed in PBS with a solution of 0.2% Tween-20 for 1 hour. Secondary antibody either to rabbit or mouse depending on the primary antibody was then added at a dilution of 1:3000, followed by an additional wash step for 1 hour. Proteins were detected either via enhanced chemiluminescence or Odyssey infrared systems. Enhanced chemiluminescence expression was performed using a combination of two developing solutions made in the lab. Solution 1 contained 100 mM Tris-HCl (pH 8.5), 2.5 mM 3-aminophthalhydrazide (Luminol; Sigma-Aldrich #A-8511) and 0.4 mM P-coumaric acid (Sigma-Aldrich #C-9008) was kept from exposure to light. Solution 2 contained 100 mM Tris-HCl (pH 8.5) and H<sub>2</sub>O<sub>2</sub> (stock 30%) at a final concentration of 0.02%. The combination of solution 1 and 2 was then added to the membrane and exposed to film.

Primary and secondary antibodies used in immunoblot analyses include those from Abcam (Cambridge, United Kingdom) recognizing eIF2 $\alpha$ -P (ab32157), and from Cell Signaling Technology (Danvers, MA) antibodies for Actin (#8457). Antibodies for GADD34 (sc-8327) and CHOP (sc-7351) were purchased from

Santa Cruz Biotechnology (Santa Cruz, CA). The eIF2 $\alpha$  total antibody was a kind gift from the laboratory of Dr. Scot Kimball (Pennsylvania State University Medical School). ATF6 antibody was prepared in rabbits using the mouse ATF6 N-terminal amino acid residues 6-307 as the antigen and was used at a concentration of 1:250 in 5% milk powder in PBS with 0.2% Tween20, as previously described [25]. ATF4 and ATF5 antibodies were prepared against the corresponding recombinant human proteins, which were affinity purified. Secondary antibodies were purchased from BioRad (Hercules, CA). The Odyssey infrared imaging system (LI-COR, Lincoln, NE) was used to visualize actin, total eIF2 $\alpha$ , and CHOP antibodies. Protein levels were measured by densitometry using the program ImageJ [90].

Flash frozen liver tissue samples were prepared for immunoblot analysis through homogenization via sonication in 1 ml of RIPA. Lysates were then clarified by centrifugation at 13,000 x g for 30 minutes. Supernatants were analyzed via the Lowry assay. Equal concentrations of proteins were separated by electrophoresis in an SDS-polyacrylamide gel, followed by transfer to nitrocellulose membranes, blocking with 5% nonfat powder milk, and overnight incubation with primary antibody as described above. The methods of detection for liver samples were the same as those for cell culture. Liver samples required a higher primary antibody concentration for protein detection compared to proteins lysates prepared from cell culture.



### **2.3 Interpreting the observed induction of eIF2 $\alpha$ -P and the UPR activation during ER stress.**

eIF2 $\alpha$  phosphorylation can occur via one of four protein kinases, and the downstream effectors activated vary depending on the type of stress. It is important to use control measurements of UPR or nutrient starvation to confirm that the expected stress pathway is activated by the experimental stress condition. For example, induction of ATF6(N) or XBP1s is thought to be restricted to ER stress. ATF6 cleavage and detection of ATF6(N) is thought to occur upon disruption of the ER. Induction of ATF6 mRNA, however, can occur in response to nutritional stresses, so care must be taken to ensure detection of ATF6(N) via immunoblot analysis (Figure 3-1B, 3-3A). Induction of XBP1s, which is a consequence of activation of IRE1 in response to ER stress, is absent or even repressed in response to nutritional stress, making it another excellent marker of ER stress (Figure 3-1A, 3-3A).

### **2.4 Animals**

Animal protocols were approved by the Institutional Animal Care and Use Committees at Rutgers, The State University of New Jersey and Indiana University School of Medicine, Indianapolis, IN. Whole Body ATF4 knockout mice (WbATF4-KO) were described [78] and obtained from the Jackson Laboratory (Bar Harbor, Maine). C57BL/6J mice homozygous for the *LoxP* allele of *ATF4* (*ATF4<sup>fl/fl</sup>*) [91] were bred with C57BL/6J mice heterozygous for the Cre recombinase gene under an albumin gene promoter (*AlbCre*) to create

a liver-specific knockout of *ATF4*, LsATF4-KO (*AlbCre*<sup>-\*</sup> *ATF4*<sup>fl/fl</sup>). Cre-negative mice from these litters expressed WT levels of *ATF4* and were used as controls. Genotyping showed efficient *ATF4* gene deletion, and proteins level reductions were seen in response to Tm treatment (Figures 5, A and E). Female adult mice (n = 5-8 per treatment group), aged 3 to 6 months were individually housed in plastic cages with soft bedding, maintained on 12 hour light/dark cycles, and freely provided tap water and commercial pelleted diet (5001 Laboratory Rodent Diet, LabDiet). Mice received intraperitoneal (IP) injections of tunicamycin at a dose of 1 mg/kg body weight, whereas control mice were given a vehicle consisting of a solution of 0.3% dimethyl sulfoxide (DMSO) in phosphate-buffered saline. Mice were killed by decapitation using a rodent guillotine at 6, 24, and 36 hours after treatment, as indicated. Livers were rinsed with ice-cold PBS and then snap frozen in liquid nitrogen or fixed in 4% paraformaldehyde. Mice homozygous for the *LoxP* allele of *PERK* (*PERK*<sup>fl/fl</sup>) were previously described [25] and were bred with transgenic mice heterozygous for the Cre recombinase gene under an albumin gene promoter (*AlbCre*) to create a liver-specific knockout of *PERK*, LsPERK-KO (*AlbCre*<sup>-\*</sup> *PERK*<sup>fl/fl</sup>). Cre-negative mice from these litters expressed WT levels of *PERK* and were used as controls.

## 2.5 Reverse Transcription and Real-Time PCR

Total RNA was extracted from cultured Hepa1-6 and MEF cells and from liver tissues by using TRIzol reagent (Life Technologies, Grand Island, NY)

following the manufacturer's instructions, which yielded preparations with  $A_{260}/A_{280}$  ratios between 1.8 and 2.0 as observed by spectrophotometry.

Reverse transcription was performed with 1  $\mu$ g of each RNA sample using the High-Capacity cDNA Reverse Transcription Kit (Applied Biosystems, Foster City, CA) according to the manufacturer's instructions. Levels of the indicated mRNAs were determined by qPCR. Primers used for SYBR Green are listed in Table 2-1. Amplification and detection were measured on the Realplex<sup>2</sup> Master Cycler (Eppendorf, Hauppauge, NY). All experiments were performed with at least 3 biological replicates and with technical replicates. Results were generated using comparative  $C_t$  method and are expressed as fold change relative to the untreated control.

**Table 2-1. Sequence of Primers for SYBR green based qRT-PCR.**

<b>Name</b>	<b>Forward</b>	<b>Reverse</b>
Abca1	AACAGTTTGTGGCCCTTTTG	AGTTCAGGCTGGGGTACTT
Abcg5	CGTCCAGAACAACACGCTAA	GCAGCATCTGCCACTTATGA
Abcg8	AAGACGGGCTGTACACTGCT	AGGAGGACATGTGGAAGGTG
Actin	TGTTACCAACTGGGACGACA	GGGGTGTGAAGGTCTCAA
ASNS	TTGACCCGCTGTTTGGAAATG	CGCCTTGTGGTTGTAGATTTTAC
ATF4	GCCGGTTTAAGTTGTGTGCT	CTGGATTCGAGGAATGTGCT
ATF5	GGCTGGCTCGTAGACTATGG	CCAGAGGAAGGAGAGCTGTG
ATF6	GATGCAGCACATGAGGCTTA	CAGGAACGTGCTGAGTTGAA
BiP	TGCAGCAGGACATCAAGTTC	TACGCCTCAGCAGTCTCCTT
CHOP	CGGAACCTGAGGAGAGAGTG	CGTTTCCTGGGGATGAGATA
CTH	TGCTAAGGCCTTCCTCAAAA	AAGCTCGATCCAGGTCTTCA
CYP7A1	ACACCATTCTGCAACCTTC	GCTGTCCGGATATTCAAGGA
CYP27A1	TCTGGCTACCTGCACTTCCT	CTGGATCTCTGGGCTCTTTG
FGF21	AGATGGGCTCTCTATGGATCG	GGGCTTCAGACTGGTACACAT
GADD34	AGGACCCCGAGATTCTCTA	CCTGGAATCAGGGGTAAGGT
HNF4a	GGTCAAGCTACGAGGACAGC	ATCCAGAAGGAGTTCGCAGA
nCEH1	TTCTGGAGACAGTGCTGGTG	GGATCGGAGTGTTTCATGCTT
SOAT2	GTGCCTGGGATCTTTTGTGT	GGATGAAGCAGGCATAGAGC
SOD2	CCGAGGAGAAGTACCACGAG	GCTTGATAGCCTCCAGCAAC

XBP1t	AAGAACACGCTTGGGAATGG	ACTCCCCTTGGCCTCCAC
XPB1s	GAGTCCGCAGCAGGTG	GTGTCAGAGTCCATGGGA

## 2.6 Histology

Tissues were fixed in 4% paraformaldehyde, frozen, and then sectioned at 10  $\mu\text{m}$ , using a cryostat. TUNEL assays were performed according to the manufacturer's instructions (Trevigen TACS 2 TdT-Blue Label In Situ Apoptosis Detection Kit; R&D System, Minneapolis, MN). TUNEL- positive cells were measured from equally sized sections of livers derived from a similar location within the tissues. Digital images of the selected areas were prepared at 200x and imported into Scion Image for Windows (Scion Corporation, Frederick, MD), and TUNEL-positive cells were manually marked and counted.

## 2.7 Cholesterol Measurements

Cholesterol content was measured in lysates prepared from liver tissues by using the Amplex Red Cholesterol assay kit (Molecular Probes, Eugene, OR). Cholesterol standards, liver lysate samples, and resorufin positive control were placed into a 96 well plate in a volume of 50  $\mu\text{l}$  (100  $\mu\text{l}$  for the resorufin) per well, prior to the addition of the working solution of 300  $\mu\text{M}$  Amplex Red reagent. Plates were then incubated for 30 minutes at 37°C, protected from light sources. Resorufin, the product of the amplex red reagent, was then measured in a Synergy H1 (BioTek, Winooski, VT) fluorescence microplate reader using excitation at 530 nm and emission detection of 590 nm. Fluorescence intensity

was then used to calculate the amount of cholesterol ( $\mu\text{g}$ ) based on the standard curve, which was normalized for protein concentrations determined for lysates.

## **2.8 RNA-Seq Analysis**

WT and LsATF4-KO mice were injected IP with 1 mg/kg tunicamycin or vehicle for 6 hours and total RNA was prepared with TRIzol reagent (Life Technologies, Grand Island, NY) following the manufacturer's instructions by our collaborators at Rutgers University. RNA sequencing was performed using an Illumina HiSeq2000 at Columbia University (Sulzberger Genome Center), with single-end reads and a read length of 100 base pairs. Real-Time Analysis (RTA) was used for base-calling. Fastq files were mapped to the mouse genome (NCBI37/mm9) using TopHat (v2.0.4). Mapped reads were then assembled via Cufflinks (v2.0.2) with the default settings. Assembled transcripts were then merged using the Cuffmerge program with the reference genome. Analysis of mRNA levels was carried out using the Cuffdiff program, with samples being grouped by treatment condition, giving 4 conditions and 3 replicates per group. Samples were considered if they demonstrated a fold change between WT NT and WT Tm of 1.5 or greater, and if their q-value, a False Discovery Rate (FDR) adjusted p-value with FDR set at 0.05, was less than or equal to 0.05. Venn diagrams were created with the use of a Venn diagram program (Venny 2.0.2) available at the following link (<http://bioinfogp.cnb.csic.es/tools/venny/>). RNA-Seq data are deposited in Gene Expression Omnibus ([www.ncbi.nlm.nih.gov/geo/](http://www.ncbi.nlm.nih.gov/geo/)) under the series number (GSE76771).

## **2.9 PANTHER Overrepresentation Test**

PANTHER overrepresentation test (<http://pantherdb.org/>) compares the input gene list against a reference list. A list of genes altered by the loss of ATF4 under basal and stress conditions were used as inputs. The reference list consisted of the PANTHER-GO list of mouse genes. Lists of genes targeted by ATF4 were then subdivided by the same categories as the PANTHER list, on the basis of GO classification, and then a binomial test was performed to determine overrepresentation of the user list of genes compared to expected number of genes if occurring at random. Results were evaluated with a Bonferroni corrected p-value. P-values less than 0.05 were considered significant.

## **2.10 Generation of Volcano Plots**

Results from the RNA-Seq analysis for each condition comparison; WT NT to Tm, WT NT to LsATF4-KO NT, and WT Tm to LsATF4-KO Tm were read into R studio. The fold change and q-value for each gene were then represented on a volcano plot using the code listed in Table 2-2. R (v3.1.1) was used with the only additional library required being the calibrate library. Images were then transferred into Adobe Illustrator for editing.

**Table 2-2. Code for Generation of Volcano Plots**

```
Volcano2NoLabLeg <- function(filename, Treatment) {  
  rna <- read.table(filename, header = TRUE, fill = TRUE)  
  rna2 <- transform(rna, log10pvalue = -log10(p_value))  
  with(rna2, plot(log2.fold_change., log10pvalue, pch =20, col = rgb(0,0,0,alpha =  
0.2)))  
  with(subset(rna2, q_value<0.05), points(log2.fold_change., log10pvalue, pch =  
20, col = rgb(1,0,0,0.2)))  
  with(subset(rna2, abs(log2.fold_change.)>0.5), points(log2.fold_change.,  
log10pvalue, pch = 20, col = rgb(0,0.39,0,0.2)))  
  with(subset(rna2, q_value<0.05 & abs(log2.fold_change.)>.5),  
points(log2.fold_change., log10pvalue, pch = 20, col = rgb(1,0.84,0,0.2)))  
  with(subset(rna2, q_value<0.05 & abs(log2.fold_change.)>.5 & gene == "Ddit3"),  
points(log2.fold_change., log10pvalue, pch = 18, col = "Black"))  
  with(subset(rna2, q_value<0.05 & abs(log2.fold_change.)>.5 & gene == "Atf4 "),  
points(log2.fold_change., log10pvalue, pch = 15, col = "Black"))  
  with(subset(rna2, q_value<0.05 & abs(log2.fold_change.)>.5 & gene == "Asns"),  
points(log2.fold_change., log10pvalue, pch = 17, col = "Black"))  
}
```

## 2.11 Lipid Peroxidation measurements

The Lipid Peroxidation (MDA) Colorimetric/Fluorometric Assay from BioVision (BioVision, Milpitas, CA) was used to measure the natural by-product of lipid peroxidation malondialdehyde (MDA). Liver tissue was obtained from

LsPERK-WT, LsPERK-KO, LsATF4-WT, and LsATF4-KO mice that were treated with 0.3% DMSO or 1 mg/kg tunicamycin for 24 hours prior to livers being collected. 10 mg of liver tissue or cell culture was prepared in MDA lysis buffer and then sonicated prior to centrifugation. Cell lysate protein was calculated via Lowery assay to allow normalization of samples per mg of protein used. The MDA-TBA adduct was colorimetrically detected at ( $\lambda = 532\text{nm}$ ), and the MDA concentration was adjusted according to the mass of liver tissue used for each sample and the standard curve based on a provided MDA standard prepared in serial dilutions. Samples were measured on a Synergy H1 (BioTek, Winooski, VT) fluorescence microplate reader.

## **2.12 Measurements of Mitochondrial Membrane Potential**

15,000 Hepa1-6 shCtrl and Hepa1-6 shATF4 cells were plated per well in a 96 well plate. Cells were treated with vehicle or 2  $\mu\text{M}$  rotenone for 6 hours. The media was removed and 100  $\mu\text{l}$  of Mitotracker Red (ThermoFisher, Waltham, MA) was added to serum free DMEM plus 10  $\mu\text{g/ml}$  Hoechst stain (ThermoFisher, Waltham, MA). The cells were incubated at 37°C for 1 hour, prior to removing the probes and washing twice with DMEM. The cells were then imaged using spinning disk confocal microscopy using Opera (PerkinElmer, Waltham, MA) and quantified using the program Columbus as previously described [89].

## **2.13 Luciferase assays**



Luciferase assays were carried out in six-well plates with the Dual-Luciferase reporter assay system according to the manufacturer's instructions (Promega, Madison, WI). The plasmid p5XATF6GLC3 used for measuring ATF6 activity plasmid was provided by Dr. Ron Prywes (Columbia University) and was previously described [92]. This reporter contains five ATF6 binding elements integrated into a promoter adjoined to the firefly luciferase reporter gene and was cotransfected into Hepa1-6 cells, along with a *Renilla* expressing plasmid for normalization. Measurements were determined as the relative light units (RLU) of the firefly luciferase to the *Renilla* luciferase.

**Table 2-3. Plasmids used in this study**

<b>WB ID#</b>	<b>Description</b>	<b>Source</b>
912	5X ATF6 in pGL3 luciferase. Contains 5 optimized ATF6 binding elements in tandem.	Prywes
984	pMDLg/pRRE Lenti (packaging) from Addgene 3 <sup>rd</sup> generation plasmids, AmpR	Cornetta
985	pRSV-REV Lenti(packaging) from Addgene 3 <sup>rd</sup> generation plasmids, AmpR	Cornetta
986	pVSV-G Lenti (envelope) from Addgene 3 <sup>rd</sup> generation plasmids, AmpR	Cornetta
1175	shRNA Control, AmpR	Quilliam
1180	shRNA mATF4 TRC identifier (last 2-digits) #26, AmpR	Sigma-Aldrich
1181	shRNA mATF4 TRC identifier (last 2-digits) #27, AmpR	Sigma-Aldrich
1162	shRNA mATF5 TRC identifier (last 2-digits) #56, AmpR	Sigma-Aldrich
1164	shRNA mATF5 TRC identifier (last 2-digits) #53, AmpR	Sigma-Aldrich
1173	shRNA mATF6 TRC identifier (last 2-digits) #26, AmpR	Sigma-Aldrich

1174	shRNA mATF6 TRC identifier (last 2-digits) #28, AmpR	Sigma-Aldrich
1246	shRNA mCHOP TRC identifier (last 2-digits) #09, AmpR	Sigma-Aldrich
1247	shRNA mCHOP TRC identifier (last 2-digits) #77, AmpR	Sigma-Aldrich

## 2.14 Cell Survival Assays

The Calcein AM Viability Dye (eBioscience, San Diego, CA) was used to measure cell survival. This assay was performed in 96 well plates and evaluated according to manufacturer's instructions using a Synergy H1 (BioTek, Winooski, VT) reader with an excitation wavelength of 495 nm and emission detection at 515 nm.  $5 \times 10^3$  cells were cultured in DMEM supplement with 10% FBS, penicillin (100 IU/ml), and streptomycin (100  $\mu$ g/ml) in a final concentration of 2  $\mu$ M tunicamycin, 1  $\mu$ M MG132, or no stress agent for 24 hours. Calcein-AM dye was then added for 30 minutes at room temperature prior to measuring fluorescence. The Caspase 3/7 kit was carried out using the Caspase-Glo 3/7 kit (Promega, Madison, WI) that was performed in 96 well plates, as previously described [93]. Briefly, livers were homogenized in a hypotonic extraction buffer (25 mM HEPES (pH 7.5), 5 mM  $MgCl_2$ , 1 mM EGTA, 1 mM PMSF, and 1  $\mu$ g/ml of aprotinin, leupeptin, and pepstatin). The liver lysates were then clarified by centrifugation at 13,000 x g for 30 minutes at 4 °C. Equal volumes of the diluted extracts (10  $\mu$ g/ml) and Caspase-Glo reagent were used in the 96 well plates, prior to 1-hour incubation at room temperature. Results were then read using a Synergy H1 plate reader.

## 2.15 Statistics

All data are shown as the mean  $\pm$  SD and were derived from at least 3 independent experiments. Statistical significance was determined using the two-tailed Student's *t*-test.

Multiple testing between groups was assessed using a two-way analysis of variance to determine the significance of the interaction between the groups. The “\*” indicates statistical significance ( $p < 0.05$ ) with respect to the treated samples between the two cell types. The “#” highlights statistical significance ( $p < 0.05$ ) with respect to the untreated samples between the two cell types. The “\$” indicates statistical significance ( $p < 0.05$ ) between untreated sample compared to ER stress for each cell type.

## CHAPTER 3. RESULTS: THE ISR IS REQUIRED FOR ATF6 ACTIVATION

### 3.1 UPR signaling differs between cell culture models

UPR studies featuring MEF cells subjected to pharmacological induction of ER stress indicated that ATF4 directs transcriptional expression of genes involved in amino acid metabolism, oxidative stress reduction, and control of apoptosis [6]. To address the role of ATF4 in the UPR in hepatocytes, we depleted *ATF4* expression in the mouse hepatoma cell line Hepa1-6 using shRNA and compared the induction of key UPR genes with that of MEF cells deleted for ATF4 (Figure 3-1, A-D). There was a significant reduction in *ATF4* mRNA and protein in the shATF4 cells compared to control after 3 or 6-hour treatment with 2  $\mu$ M tunicamycin (Tm), an inhibitor of N-glycosylation of proteins in the ER and potent inducer of ER stress (Figure 3-1, C and D). Known ATF4-target genes involved in amino acid metabolism, including *ASNS* and *FGF21*, were also found to be reduced in the Hepa1-6 cells [43, 48, 94, 95]. Hepa1-6 and MEF cell lines both demonstrated the expected increased levels of *ASNS*, *FGF21*, and *CTH* mRNAs in response to Tm, and this induction was significantly ablated upon loss of *ATF4* (Figure 3-1, A and C). Basal levels of genes were also significantly reduced upon the loss of ATF4. Differences in the gene transcripts between ATF4 loss and treatment were found to be significant by two-way ANOVA ( $p < 0.05$ ). Emphasizing the importance of cross-regulation in the UPR, ATF4 was also required for full induction of *XBP1t* mRNA and its spliced variant *XBP1s* during ER stress (Figure 1, A and C). In both MEF and Hepa1-6

cell lines, two-way ANOVA demonstrated statistical significance for the interaction between treatment and presence or depletion of *ATF4* expression.

Our comparison between ATF4-directed gene expression in Hepa1-6 and MEF cell lines also showed key differences between the two cell types. ATF4 is required for full cleavage to the active N-terminal version ATF6(N) in MEF cells treated with Tm [25]. As previously shown, the loss of *ATF4* in the MEF cells led to a reduction in full-length ATF6 protein by 67% at 6 hours, with a more pronounced 97% reduction of ATF6(N) (Figure 3-1B). However, the role of ATF4 in the activation of ATF6(N) was much diminished in Hepa1-6 cells (Figure 3-1D). In the case of *SOD2*, encoding superoxide dismutase 2 that serves to clear ROS from mitochondria, deletion of *ATF4* in MEF cells led to higher levels of *SOD2* mRNA in both basal and ER stress conditions, whereas loss of *ATF4* expression in Hepa1-6 cells led to a substantial lowering of *SOD2* transcripts in either stressed or non-stressed conditions.

Given the reported anti-oxidation role of ATF4 in MEF cells [6], we also addressed whether there was generation of oxidative stress in the Hepa1-6 cells upon loss of ATF4. We assessed the oxidation status in shATF4 and control cells by measuring malondialdehyde (MDA), which is generated by lipid peroxidation. Lipid peroxidation occurs when free radicals remove electrons from lipids [96]. Loss of ATF4 results in cellular damage [6]. MDA occurs as a natural by-product of the reaction, making it an effective marker of lipid peroxidation [96]. Depletion of *ATF4* in Hepa1-6 cells grown in DMEM, which features high levels of glucose, did not affect the accumulation of MDA (Figure 3-1E). We also

examined mitochondrial function by using the Mito Tracker Red assay to measure mitochondrial membrane potential. There was over a 2-fold reduction in the mitochondrial potential upon depletion of *ATF4*, which was similar to the lowered levels generated by treatment with rotenone, a potent inhibitor of mitochondrial respiration, which functions by inhibiting the transfer of electrons from complex 1 to ubiquinone (Figure 3-1F).

CHOP is considered to be a canonical downstream effector of the PERK/ATF4 pathway and as expected, we observed a sharp increase in *CHOP* mRNA and protein levels in MEF cells treated with Tm, which was significantly lowered upon deletion of *ATF4* (Figure 3-1, A and B). However in Hepa1-6 cells the substantial increase in *CHOP* transcripts observed during ER stress was only modestly lowered upon depletion of *ATF4*, and there was full induction of CHOP protein even with depleted *ATF4* expression (Figure 3-1, C and D). These results suggest that many features of the UPR gene expression networks described in MEF cells cannot be applied to every cell type and that UPR regulators other than *ATF4* can contribute to *CHOP* expression.

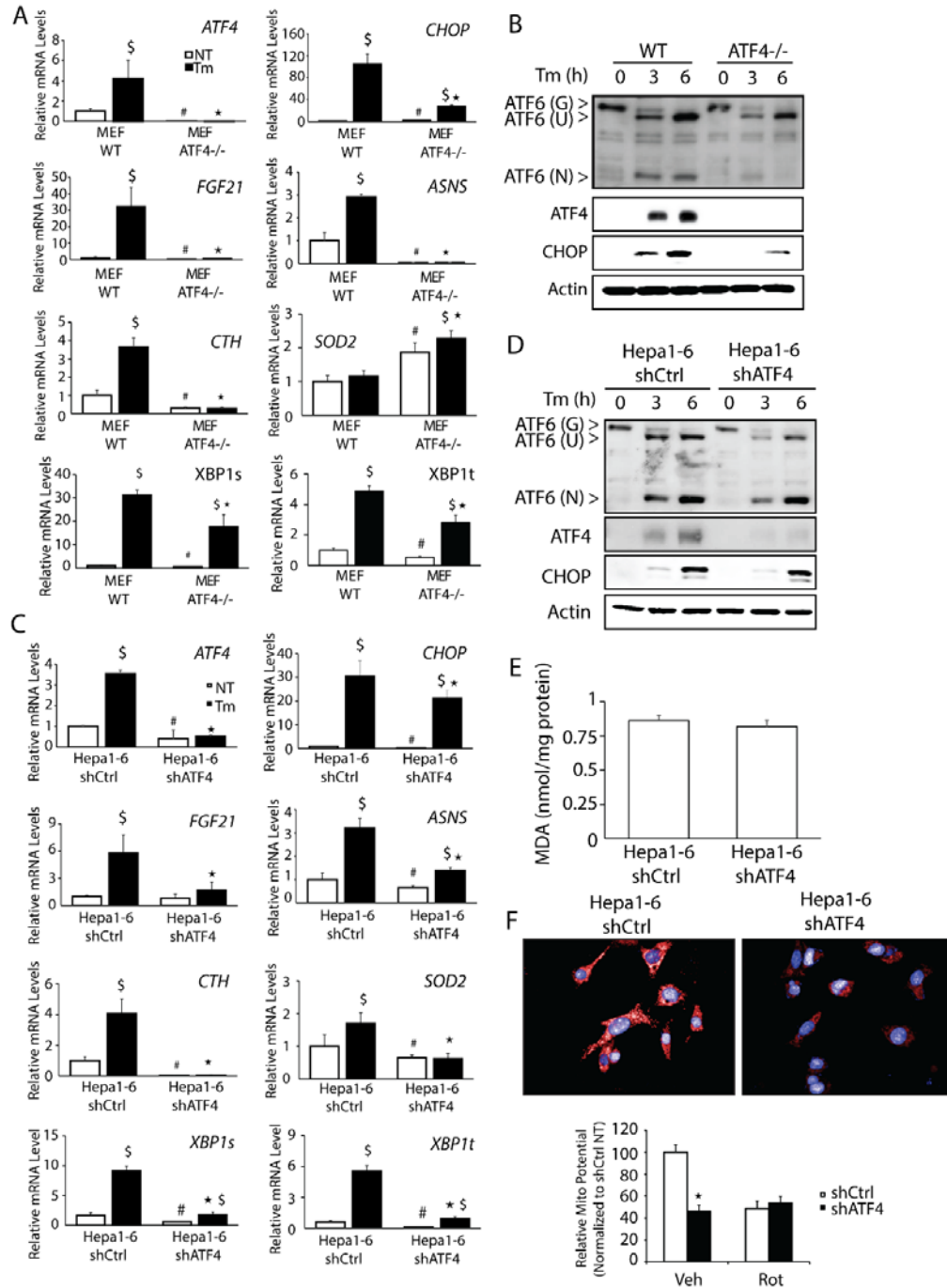


**Figure 3-1. Hepa1-6 cells demonstrate an ATF4-Independent CHOP expression.** (A) WT and *ATF4*<sup>-/-</sup> MEF cells were treated with 2  $\mu$ M tunicamycin (Tm) for 6 hours, or no stress treatment (NT) and levels of *ATF4*, *CHOP*, *FGF21*, *ASNS*, *CTH*, *SOD2*, *XBP1t*, and *XBP1s* mRNAs were determined by qPCR. (B)

WT and *ATF4*<sup>-/-</sup> MEF cells were treated with 2  $\mu$ M Tm for 3 or 6 hours and ATF4 and CHOP levels were evaluated by immunoblot analyses using specific antibodies. Levels of the indicated mRNAs (C) and proteins (D) were measured in Hepa1-6 shCtrl and Hepa1-6 shATF4 cells by qPCR and immunoblot analyses, respectively. (E) MDA analyses on Hepa1-6 shCtrl and shATF4 cells were examined using the BioVision Lipid Peroxidation kit. (F) Hepa1-6 and Hepa1-6 shATF4 cells were plated on glass bottom plates, and then evaluated using Mitotracker Red. Image of the red-fluorescent dye that stains mitochondria in live cells are shown in the top panel and quantitation are indicated by histograms in the bottom panel. The “\*” indicates statistical significance ( $p < 0.05$ ) with respect to the treated samples between the two cell types. The “#” highlights statistical significance ( $p < 0.05$ ) with respect to the untreated samples between the two cell types. The “\$” indicates statistical significance ( $p < 0.05$ ) between untreated sample compared to ER stress for each cell type.



### 3.2 Liver cell culture requires ATF6 for optimal *CHOP* expression

A previous study of CHO and COS-1 cell lines suggested that ATF6 can contribute to *CHOP* expression by an Endoplasmic Reticulum Stress Response Element (ERSE) situated in the *CHOP* promoter [53]. We addressed the role played by ATF6 in *CHOP* expression in Hepa1-6 cells by depleting ATF6 using shRNA, followed by treatment with 2  $\mu$ M Tm. Loss of ATF6 led to reductions in the expression of well-defined ATF6-target genes, including ER chaperone *BiP* (*GRP78/HSPA5*) and *XBP1t* and its spliced variant *XBP1s* (Figure 3-2A) [15, 97]. The interaction between loss of ATF6 and treatment was found to be significant by two-way ANOVA for all three genes. *ATF4* mRNA levels were also modestly reduced in the *ATF6*-depleted cells treated with Tm, but there was no measurable reduction in ATF4 protein levels (Figure 3-2, A and B). Of importance, depletion of *ATF6* sharply lowered the induction of *CHOP* mRNA and protein upon ER stress in the Hepa1-6 cells. CHOP protein levels were reduced by 76% and 51% at 3 and 6 hours, respectively. These results suggest that ATF6 can be a major contributor to *CHOP* expression, especially during ER stress. To address whether other ATF transcription factors regulated by PERK can also effect *CHOP* expression, we depleted *ATF5* expression in Hepa1-6 cells using shRNA and found no changes in induced expression of CHOP protein by ER stress (Figure 3-2C). These findings indicate that the requirement of ATF6 for induced *CHOP* expression in the Hepa1-6 hepatocytes is not broadly shared between other transcription factors, such as ATF5, which are controlled by PERK.

CHOP can direct the expression of genes involved in protein homeostasis, in particular, those promoting protein folding, such as *HSPA1B* and *DNAJ4*, and a number of aminoacyl tRNA-synthetases, including *WARS* [51, 54, 55, 98]. By contrast during prolonged ER stress triggered by pharmacological agents, CHOP can instead trigger cell death through the expression of pro-apoptotic genes such, as *BIM* or *GADD34* [51, 55, 98-100]. We wished to determine whether depletion of the upstream regulators ATF6 or ATF4 altered Hepa1-6 survival upon treatment with either Tm or another stress agent, the proteasome inhibitor MG132. As expected, in Hepa1-6 cells depletion of *CHOP* showed protective effects upon either stress treatment as judged by lowered calcein-AM labeling (Figure 3-2D). Lowered expression of either *ATF4* or *ATF6* led to significant increases in cell death upon ER stress, 20%, and 15% respectively, compared to control cells. These findings are consistent with the protective effects attributed to the ATF4 and ATF6 transcription factors in the UPR [6, 21].

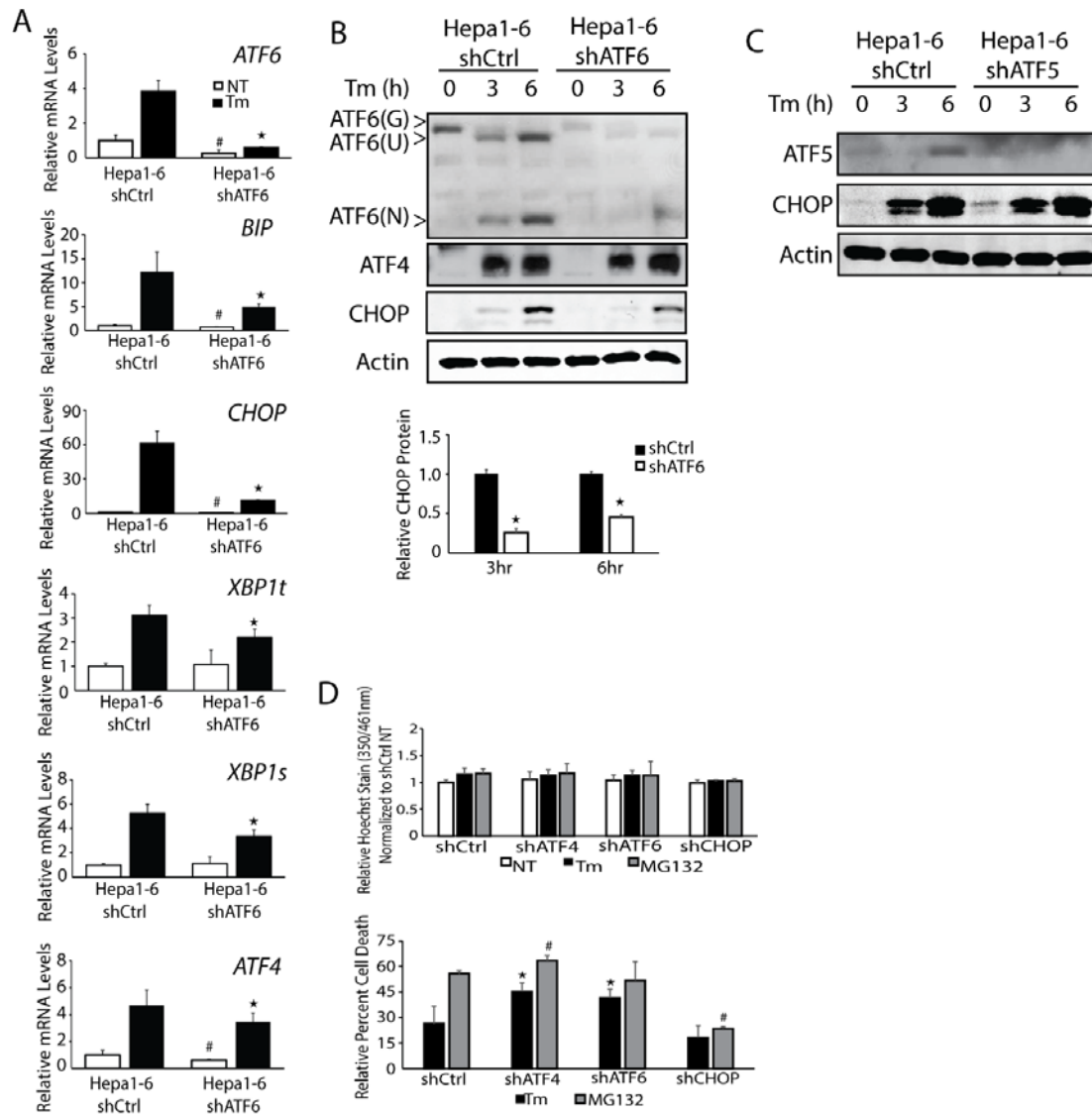


**Figure 3-2. ATF6 facilitates induced *CHOP* expression in liver cells**

**subjected to ER stress.** (A) Hepa1-6 shCtrl and Hepa1-6 shATF6 cells were treated with 2  $\mu$ M tunicamycin (Tm) for 6 hours, or no stress treatment (NT), and the levels of *ATF4*, *CHOP*, *ATF6*, *XBP1t*, *XBP1s*, and *BiP* mRNAs were determined by qPCR. (B) Hepa1-6 shCtrl and Hepa1-6 shATF6 cells were treated with 2  $\mu$ M Tm for 3 or 6 hours and *ATF4*, *ATF6*, and *CHOP* levels were evaluated by immunoblot analyses. *CHOP* levels were quantified using ImageJ based on three independent experiments for the 3 and 6 hour time points. (C)

Hepa1-6 shCtrl and Hepa1-6 shATF5 cells were treated with 2  $\mu$ M Tm for 3 or 6 hours and levels of ATF5 and CHOP proteins were measured by immunoblot analyses. (D) Hepa1-6 shCtrl, shATF4, shATF6, and shCHOP cells were treated with 2  $\mu$ M Tm or 1  $\mu$ M MG132 for 24hrs, or no stress treatment. Cell proliferation was analyzed via Hoechst fluorescence, and cell death was measured by calcein fluorescence. The “\*” indicates statistical significance ( $p < 0.05$ ) with respect to the treated samples between the indicated cell types, and “#” indicates with respect to the untreated samples between the cell types.

### 3.3 Both ATF4 and ATF6 drive *CHOP* expression during nutritional stress

We next addressed whether ATF4 and ATF6 contribute to *CHOP* expression in response to a stress that does not directly perturb the ER. Halofuginone (HF) has been previously shown to deplete charging of tRNA<sup>Pro</sup>, leading to activation of GCN2, another eIF2 kinase, which can, in turn, enhance the transcriptional and translational expression of *ATF4* and *CHOP* [101, 102]. Treatment of Hepa1-6 cells with 50 nM HF for 6 hours led to significant increases in *ATF4* and *CHOP* mRNAs and proteins (Figure 3-3, A-C). Loss of either ATF6 or ATF4 substantially lowered both *CHOP* mRNA and protein (Figure 3-3, A-C). Expression of *GADD34* mRNA and protein was largely dependent on ATF4, with further increases in *GADD34* induction upon depletion of ATF6. It is noted that despite there being robust eIF2 $\alpha$ -P and induction of *ATF4*, *CHOP*, and *GADD34* mRNAs in response to HF, the increase in ATF4, CHOP, and GADD34 proteins were reproducibly less than Tm treatment (Figure 3-1C). This difference in the levels of induced CHOP and ATF4 proteins may be a consequence of the diminished Pro-tRNA<sup>Pro</sup> available for protein synthesis during HF treatment.

Consistent with the idea that the treatment regimen of HF did not elicit ER stress, there was no increase in the levels of *XBP1t* mRNA, and the amount of *XBP1s* transcripts were in fact substantially lowered in shCtrl Hepa1-6 cells exposed to HF. ATF6 was suggested to contribute to *CHOP* expression, and there was a 3-fold increase in *ATF6* mRNA levels during HF treatment. While we did not measure appreciable activated ATF6(N) protein upon HF treatment by

immunoblot analyses, there was a 2-fold increase in ATF6-directed transcription as measured by a luciferase reporter assay, which was significant although diminished compared to ~15-fold enhancement during Tm treatment (Figure 3D). These results suggest a model where nutrient stress afflicting the cytosol induces both ATF4 and ATF6 to contribute to increased *CHOP* expression. By comparison, ER stress triggers a pathway that is largely dependent upon ATF6 for *CHOP* expression (Figure 3-3E).

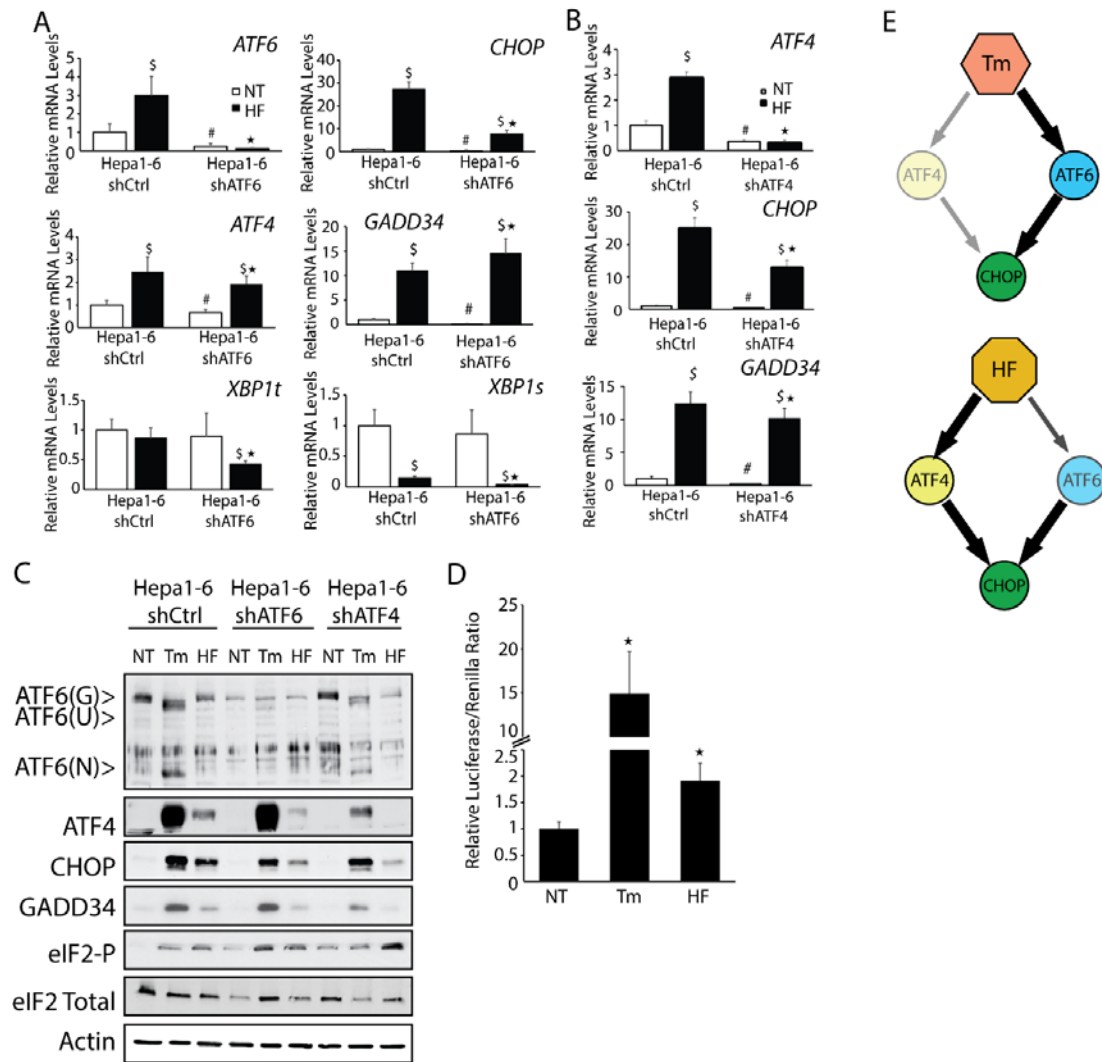


**Figure 3-3. ATF6 contributes to *CHOP* expression in multiple stresses.**

Hepa1-6 cells expressing shCtrl, shATF6, or shATF4, were treated with 2  $\mu$ M tunicamycin (Tm) or 50 nM halofuginone (HF) for 6 hours or no stress treatment (NT), as indicated. (A, B) Levels of the indicated gene transcripts were measured by qPCR. (C) The amounts of the indicated proteins were measured by immunoblot analyses. (D) Hepa1-6 cells were co-transfected with 5x ATF6 Binding Element Luciferase construct and Renilla. After 24 hours, cells were treated with 2  $\mu$ M Tm or 50 nM HF, prepared and firefly luciferase normalized for

Renilla were measured for prepared lysates. (E) Model of the roles of ATF4 and ATF6 on the expression of *CHOP* during ER stress and cytosolic stress triggered by HF treatment. The “\*” features statistical significance ( $p < 0.05$ ) between ER stress-treated cells. The “#” indicates significance ( $p < 0.05$ ) of untreated cells, and “\$”significance ( $p < 0.05$ ) of untreated cells.



### 3.4 Comparison of ATF4 and ATF4/CHOP target genes in ATF4 knockout mouse

The identification of ATF4-independent induction of *CHOP* expression in Hepa1-6 cells subjected to ER stress raises the question of whether this pattern of gene expression is physiologically relevant *in vivo*. We initially characterized whole body *ATF4*-depleted mice (WbATF4-KO), but the breeding of these animals can be problematic as reported [78] and we subsequently extended our analyses to mice with a liver-specific *ATF4* deletion (LsATF4-KO). Mice expressing Cre from the albumin promoter were bred to *ATF4* gene floxed mice in a manner similar to the liver-specific *PERK* knockout that our laboratories have previously described [25]. WbATF4-KO (Figure 3-4) and LsATF4-KO mice (Figure 3-5), and their wild-type (WT) controls were treated with 1 mg/kg Tm or 0.3% DMSO vehicle administered via an intraperitoneal (IP) injection for 6 hours. As expected *ATF4* mRNA and protein were induced upon Tm treatment in WT livers, and ATF4 was minimally expressed in either knockout model (Figure 3-4, A and E and 3-5, A and E). Consistent with the loss of ATF4 transcriptional activity, there was significant lowering in the expression of ATF4-target genes *ASNS*, *FGF21*, and *CTH* in the WbATF4-KO and LsATF4-KO livers (Figures 3-4, B and D and 3-5, B and D). Two-way ANOVA analysis indicated significance between the treatment and mouse model for *ASNS* and *FGF21* but did not achieve significance for *CTH*. This would indicate the response for *CTH* is dependent upon the loss of ATF4 within the basal state.

We next addressed the requirement for ATF4 for *in vivo* induction of key UPR gene markers. Activation of ATF6(N) protein in the liver during ER stress was largely independent of ATF4 function, and there was only modest lowering of induced *ATF6* mRNA in LsATF4-KO compared to WT (Figure 3-4, A and E and 3-5, A and E). Levels of *ATF6* mRNA in the WbATF4-KO were statistically indistinguishable. Of importance, there was only minimal lowering of induced *CHOP* mRNA upon ER stress in either model of *ATF4* depletion and full induction of CHOP protein independent of ATF4 function. Expression at WT levels of ATF6 and CHOP can also be seen in the heterozygous mice for the *ATF4*-KO (Figure 3-4E). Transcriptional expression of *GADD34* and *ATF5* are dependent on both CHOP and ATF4, and consistent with retention of CHOP function in the *ATF4* knockout models, there was a partial induction of *GADD34* and *ATF5* mRNAs compared to WT (Figure 3-4C and 3-5C). Together, these results are similar to our analyses with Hepa1-6 hepatoma cells and suggest that in the liver *CHOP* and *ATF6* expression are uncoupled from ATF4 transcriptional responsibilities in the UPR. Of importance, reported microarray analyses of livers prepared from WT and *ATF6* $\alpha$ <sup>-/-</sup> mice showed that loss of ATF6 significantly lowered *CHOP* mRNA expression basally and upon IP injection with Tm for 8 hours [21] (Figure 3-4F), a finding consistent with our UPR analyses in Hepa1-6 cells (Figure 2A).

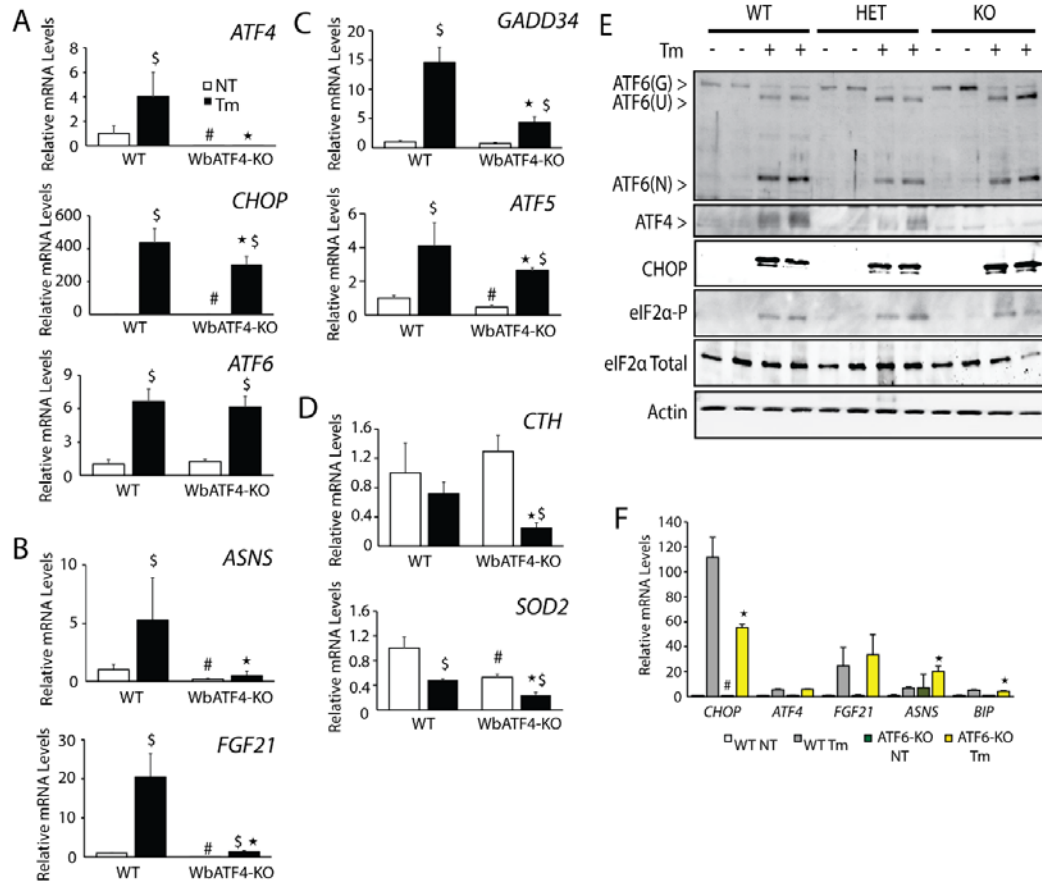


**Figure 3-4. CHOP expressed independent of ATF4 in WbATF4-KO mice.**

WT and WbATF4-KO were injected IP with 1 mg/kg body weight tunicamycin (Tm) or vehicle indicating no treatment (NT) for 6 hours. (A-D) Livers were collected and mRNA levels were measured by qPCR for the indicated genes. (B) ASNS and *FGF21* represent ATF4-target genes. (C) *GADD34* and *ATF5* highlight genes regulated by both ATF4 and CHOP. (D) *CTH* and *SOD2* were analyzed to assess genes involved in mitochondrial function and oxidative stress. (E) The indicated proteins were measured by immunoblot analyses using lysates prepared from livers derived from mice treated with DMSO (-) or Tm (+) for 6 hours. (F) Measurement of mRNAs from microarray data derived from livers of whole body ATF6 knockout mice and their WT littermates [21]. The “\*” indicates

statistical significance ( $p < 0.05$ ) among ER stress treated livers. “#” indicates statistical significance ( $p < 0.05$ ) among untreated liver tissues, and “\$” significance ( $p < 0.05$ ) with respect to the untreated and treated tissues.

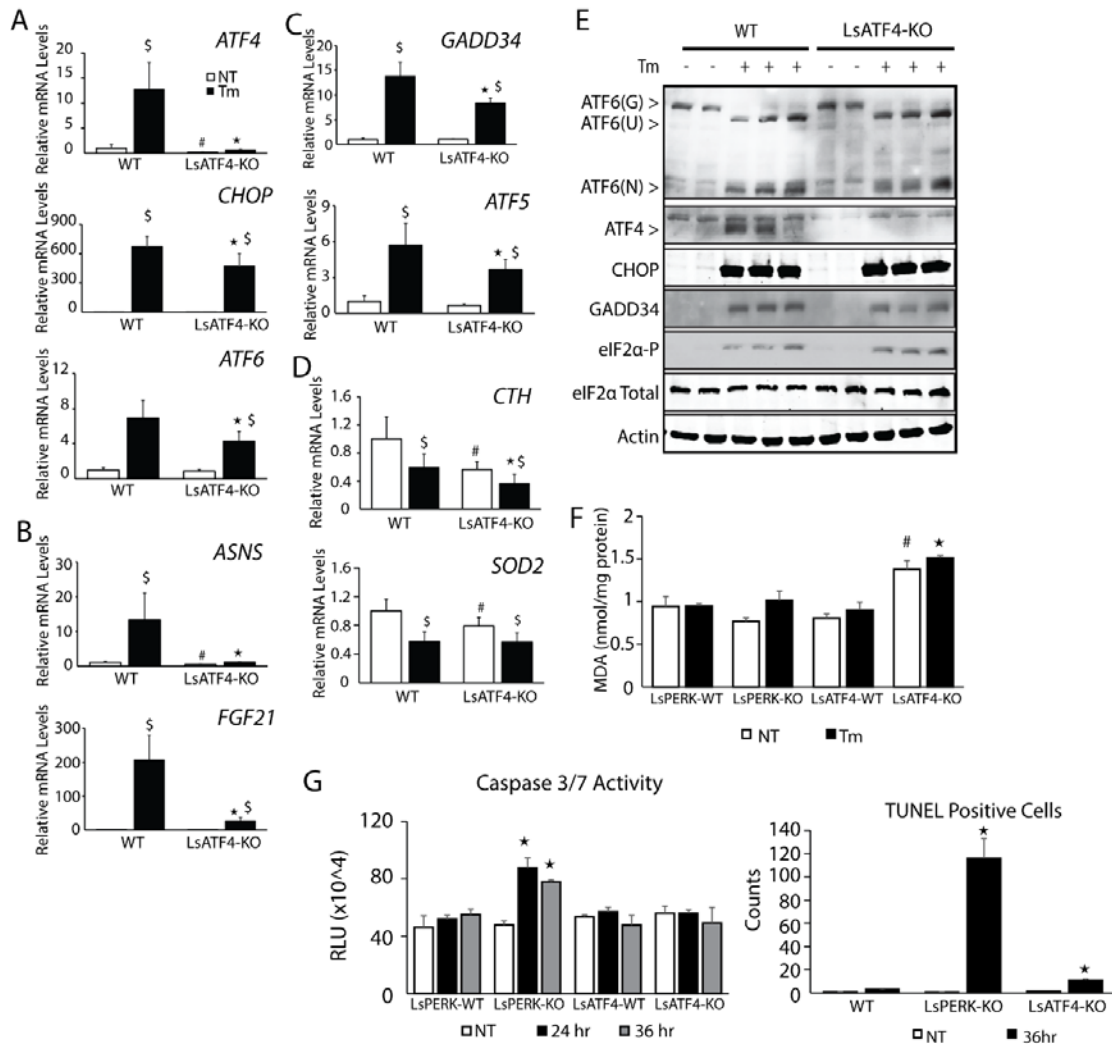


**Figure 5. CHOP is expressed independent of ATF4 in LsATF4-KO mice.**

WT and LsATF4-KO were injected IP with 1 mg/kg body weight tunicamycin (Tm) or vehicle indicating no treatment (NT) for 6 hours. (A-D) Livers were collected and mRNA levels for the indicated genes were measured by qPCR. (B) ASNS and *FGF21* are indicated ATF4-target genes, (C) *GADD34* and *ATF5* highlight genes regulated by both ATF4 and CHOP. (D) *CTH* and *SOD2* mRNAs were analyzed to assess genes involved in mitochondrial function and oxidative stress. (E) Immunoblot analyses of the indicated proteins were carried out in livers obtained from mice treated with DMSO (-) or Tm (+) for 6 hours. (F) Liver

samples from WT and LsATF4-KO mice treated with Tm for 24 hours were compared for levels of MDA via fluorescence using the Lipid Peroxidation Kit from BioVision. (G) LsPERK-WT, LsPERK-KO, LsATF4-WT and LsATF4-KO mice were treated with IP injection of 1 mg/kg Tm or vehicle for 24 or 36 hours and caspase 3/7 activity was measured. Histological samples were also assessed for TUNEL positive cells after 36 hours of Tm treatment, and the presented results are the average counts of 8 different histological sections. The “\*” indicate statistical significance ( $p < 0.05$ ) among cells subjected to ER stress, “#” features significance among untreated cells, and “\$” with respect to the untreated compared to treated tissues.

### **3.5 Loss of *ATF4* promotes oxidative stress and modest increase in cell death**

As previously seen in the Hepa1-6 shATF4 cell line, expression of *CTH* and *SOD2* mRNAs were also reduced in the absence of ATF4 in the mouse models (Figure 3-4D and 3-5D). LsATF4-KO mice also displayed elevated levels of MDA independent of stress (Figure 3-5F). Of importance, this resistance to oxidative stress *in vivo* can be conferred by basal expression of ATF4, and this protection can occur independent of PERK as the LsPERK-KO did not show significant differences in MDA levels compared to WT.

LsPERK-KO livers were previously shown to trigger cell death during extended periods of ER stress [25]. There was increased caspase 3/7 cleavage activity in LsPERK-KO mice upon treatment with 1 mg/kg Tm for 24 or 36 hours (Figure 3-5G). By comparison, LsATF4-KO livers showed no change in the caspase activity compared to WT. Livers prepared from LsPERK-KO treated with Tm also exhibited a robust increase in TUNEL positive cells, whereas LsATF4-KO showed a more moderate, but significant 10x increase compared to WT (Figure 3-5G). These results indicate that PERK provides robust protection of livers exposed to ER stress, whereas ATF4 plays a more moderate role.

### **3.6 RNA-Seq analysis of LsATF4-KO mice and ATF4 transcriptional subset**

To address the role of ATF4 in the genome-wide regulation of the UPR transcriptome, we carried out RNA-Seq analysis using livers prepared from WT and LsATF4-KO mice treated with 1 mg/kg Tm or vehicle for 6 hours. The RNA-

Seq featured single-end RNA sequencing with 100 base pair reads; approximately 32 million reads were collected for each mouse, with three animals per group. Reads were mapped to the mouse mm9 genome using TopHat [103, 104], and expression levels were characterized using Cufflinks, Cuffmerge, and Cuffdiff [104, 105]. Results were first analyzed by a volcano plot comparing the  $\log_2$  of fold change to the  $-\log_{10}$  of the q-value (Figure 3-6A). There were 4717 gene transcripts showing a significant change in WT liver upon ER stress ( $>1.5$ -fold,  $p < 0.05$ , FDR  $< 0.05$ ), with 2271 genes showing an increase and 2446 a decrease in expression. There were a total of 4364 genes showing a significant change in the LsATF4-KO liver upon ER stress. 3531 genes were altered upon ER stress in both WT and LsATF4-KO liver. In order to examine genes whose expression was significantly different during stress, we compared WT Tm to LsATF4-KO Tm genes. A total of 352 genes, or approximately 7.5% of the total UPR changes, were significantly affected by the loss of ATF4.

Key UPR target genes *ATF4*, *CHOP*, and *ASNS* were each significantly induced in the WT liver (Figure 3-6A). Consistent with our qPCR findings, the levels of *ASNS*, *FGF21*, and *CTH* were significantly lowered in the LsATF4-KO liver. By comparison, induced *CHOP* expression was not significantly affected by the loss of *ATF4* (Figure 3-6B). The limited role of ATF4 in the UPR is noteworthy compared to our earlier genome-wide analysis that nearly 50% of the gene transcripts showing significant changes in liver exposed to Tm were dependent on PERK [25]. We conclude that ATF4 is required for induction of only a portion of PERK-dependent genes. This finding suggests that there are



other PERK-driven events that are critical for regulation of the UPR-directed gene expression.

It is noteworthy that many genes required ATF4 for full expression during basal conditions, suggesting that ATF4 plays a significant role in directing the transcriptome in seemingly non-stressed conditions in the liver. There were 385 genes that were altered by the loss of *ATF4* during vehicle treatment. Pathway analysis of ATF4-targeted genes using PANTHER was performed on gene expression with a significant q-value between WT and LsATF4-KO livers during either basal or ER stress conditions (Tables 3-1 and 3-2) [106, 107]. The analysis was performed by using the PANTHER statistical overrepresentation test, which involves comparing a user input list of genes against a reference list containing all genes. These gene lists were then subdivided on the basis of GO classification, and a binomial test was then performed to determine overrepresentation of the users list of genes compared to the expected number if occurred by random. Under basal conditions, several categories demonstrated greater than 5-fold enrichment, including those representing fatty acid biosynthetic processes and fatty acid metabolic processes (Table 3-1).

Table 3-1. Pathway analysis using PANTHER of altered genes in WT and LsATF4-KO livers during non-stressed conditions.

GO Category	Mus musculus (REF)	Uploaded	Expected	Fold Enrichment	(+/-)	P-value
regulation of liquid surface tension (GO:0050828)	55	9	0.95	> 5	+	1.50E-04
cell-matrix adhesion (GO:0007160)	88	12	1.52	> 5	+	1.50E-05
fatty acid biosynthetic process (GO:0006633)	61	8	1.05	> 5	+	3.08E-03
locomotion (GO:0040011)	63	8	1.09	> 5	+	3.87E-03
fatty acid metabolic process (GO:0006631)	252	23	4.35	> 5	+	4.12E-08
steroid metabolic process (GO:0008202)	198	15	3.42	4.39	+	5.98E-04
macrophage activation (GO:0042116)	173	13	2.98	4.36	+	2.99E-03
homeostatic process (GO:0042592)	208	15	3.59	4.18	+	1.07E-03
receptor-mediated endocytosis (GO:0006898)	217	15	3.74	4.01	+	1.76E-03
cell-cell adhesion (GO:0016337)	362	22	6.24	3.52	+	1.20E-04
cell adhesion (GO:0007155)	550	31	9.49	3.27	+	3.06E-06
biological adhesion (GO:0022610)	577	31	9.95	3.11	+	8.88E-06
generation of precursor metabolites and energy (GO:0006091)	290	15	5	3	+	4.44E-02
lipid metabolic process (GO:0006629)	966	47	16.66	2.82	+	5.65E-08
endocytosis (GO:0006897)	380	18	6.55	2.75	+	3.13E-02
immune system process (GO:0002376)	1480	50	25.53	1.96	+	1.13E-03
developmental process (GO:0032502)	2468	75	42.57	1.76	+	2.01E-04
localization (GO:0051179)	2788	76	48.09	1.58	+	8.12E-03
cell communication (GO:0007154)	3175	85	54.77	1.55	+	4.81E-03
cellular process (GO:0009987)	7033	158	121.31	1.3	+	1.12E-02

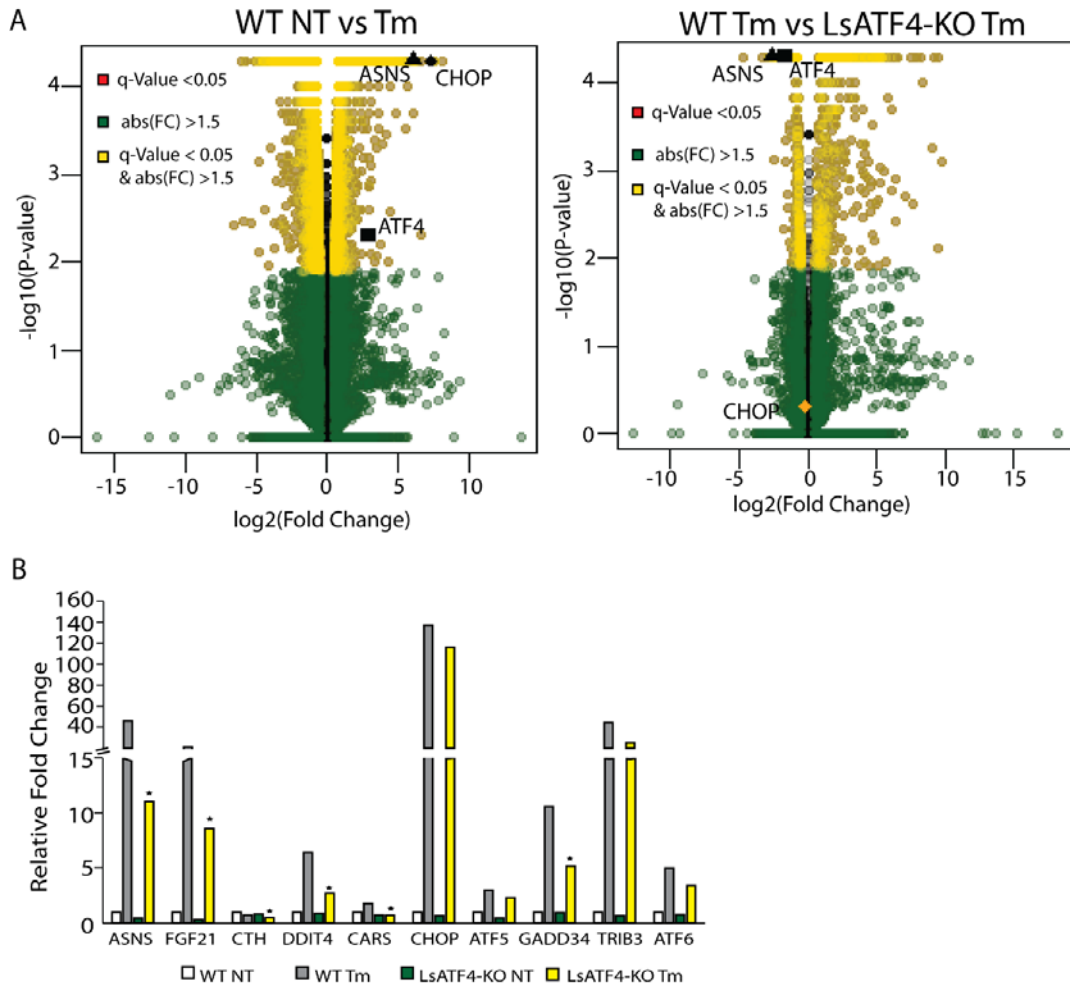
During ER stress, we identified three pathways with fold enrichment greater than 5, including steroid biosynthetic process, cholesterol metabolic process, and sterol metabolic process (Table 3-2). We also sought to further characterize the significant genes from our LsATF4-KO mice under basal and stress by comparing them to the ChiP-Seq data set, to generate altered genes that have been previously shown to be bound by ATF4 or ATF4 and CHOP [54]. Genes that were found to be significantly altered in the basal or stress states were compared with genes which were found to be bound only by ATF4 or by both ATF4 and CHOP (Table 3-3). We examined the expression levels of these ChIP-confirmed ATF4 targets in the absence of ATF4 via the RNA-Seq analysis.

Table 3-2. Pathway analysis using PANTHER of regulated genes in WT and LsATF4-KO livers during treatment with tunicamycin.

GO Category	Mus musculus (REF)	Uploaded	Expected	Fold Enrichment	(+/-)	P-value
steroid biosynthetic process	90	18	3.2	> 5	+	6.08E-05
cholesterol metabolic process	92	17	3.27	> 5	+	4.79E-04
sterol metabolic process	99	18	3.52	> 5	+	2.52E-04
cellular hormone metabolic process	74	13	2.63	4.94	+	2.84E-02
renal system process	77	13	2.74	4.75	+	4.32E-02
steroid metabolic process	194	29	6.89	4.21	+	1.67E-06
striated muscle cell development	115	17	4.09	4.16	+	1.01E-02
lipid homeostasis	111	16	3.94	4.06	+	2.79E-02
renal system development	217	31	7.71	4.02	+	1.19E-06
organic hydroxy compound biosynthetic process	142	20	5.05	3.96	+	2.56E-03
hormone metabolic process	121	17	4.3	3.95	+	1.97E-02
gland morphogenesis	114	16	4.05	3.95	+	3.88E-02
positive regulation of lipid metabolic process	122	17	4.33	3.92	+	2.19E-02
negative regulation of cellular response to growth factor stimulus	115	16	4.09	3.92	+	4.32E-02
kidney development	197	27	7	3.86	+	4.22E-05
lipid transport	206	28	7.32	3.83	+	2.64E-05
regulation of transmembrane transporter activity	172	23	6.11	3.76	+	8.59E-04
organic acid biosynthetic process	217	29	7.71	3.76	+	2.02E-05
carboxylic acid biosynthetic process	217	29	7.71	3.76	+	2.02E-05
regulation of ion transmembrane transporter activity	167	22	5.93	3.71	+	2.06E-03
monocarboxylic acid biosynthetic process	146	19	5.19	3.66	+	1.56E-02
small molecule biosynthetic process	316	40	11.23	3.56	+	1.01E-07
regulation of transporter activity	182	23	6.47	3.56	+	2.27E-03
lipid localization	233	29	8.28	3.5	+	9.35E-05

Table 3-3. Comparison of altered gene expression in the absence of ATF4 in basal and stress states with genes bound by ATF4 or both ATF4 and CHOP.

Bound by ATF4-Only vs Basal State				Bound by ATF4 and CHOP vs Basal State			
Gene	Expression in LsATF4-KO	Gene	Expression in LsATF4-KO	Gene	Expression in LsATF4-KO	Gene	Expression in LsATF4-KO
Il1r1	Up	Cr1s1	Down	Atf3	Down	Ets1	Up
Angptl4	Down	Samd8	Down	Lcn2	Up	Fam96a	Down
Ptprs	Up	Ip6k2	Down	Reln	Up	Atf5	Down
Tnfai2	Up			Uqcrcq	Down		
Bound by ATF4-Only vs Stress State							
Gene	Expression in LsATF4-KO	Gene	Expression in LsATF4-KO	Gene	Expression in LsATF4-KO	Gene	Expression in LsATF4-KO
Il1r1	Up	Slc3a2	Down	Fgf21	Down	Rhbdd1	Down
Angptl4	Down	Mras	Up	Rab39b	Down	Wwtr1	Down
Slc7a1	Down	Hax1	Down	B230217C12Rik	Down	Psat1	Down
Eif4ebp1	Down	Asns	Down	Chac1	Down	Tars	Down
Slc6a9	Down	Cars	Down	Slc25a33	Down	Pycr1	Down
Gpam	Up	Usp2	Up	Pck2	Down	Hhip1	Down
Grb10	Down	Slc1a4	Down	Scsep1	Down	Zfp608	Down
Hmox1	Down	Nupr1	Down	Ddit4	Down	Zyg11b	Down
Bound by ATF4 and CHOP vs Stress State							
Gene	Expression in LsATF4-KO	Gene	Expression in LsATF4-KO	Gene	Expression in LsATF4-KO	Gene	Expression in LsATF4-KO
Atf3	Down	Pnrc2	Down	Tsply4	Down	Paqr3	Down
Hfe	Down	Aldh18a1	Down	Zc3hav1	Down	Tbpl1	Down
Mtm1	Down	Nrip2	Down	Usp6nl	Down	Abcc4	Down
Ppp1r15a	Down	Fibin	Down	Iars	Down	Gars	Down
Slc7a5	Down	Otub2	Down	Lars	Down		
Vldlr	Down	Nars	Down	Aldh1l2	Down		
Ero1l	Down	Cyb5r1	Down	Soat2	Down		



**Figure 3-6. ATF4 is required for expression of a subset of UPR genes.** (A) RNA-Seq analyses measuring levels of gene transcripts from WT and LsATF4-KO mice treated with 1 mg/kg tunicamycin (Tm) or vehicle (NT) for 6 hours. Volcano plot of WT NT versus Tm, and WT Tm versus LsATF4-KO. (B) Levels of UPR gene transcripts by RNA-Seq analysis, which are organized into ATF4-dependent groups (*ASNS*, *FGF21*, *CTH*, *DDIT4*, and *CARS*) and those genes bound by both ATF4 and CHOP (*CHOP*, *ATF5*, *GADD34*, *TRIB3*, and *ATF6*).

### 3.7 ATF4 facilitates the metabolism of cholesterol in the liver

Given that the top three biological pathways affected during ER stress were centered on genes involved in sterol and cholesterol metabolism and *SOAT2* was an ATF4 and CHOP target, we next experimentally addressed the effect of *ATF4* loss on cholesterol. Our RNA-Seq and PANTHER Pathway analysis suggested a role for ATF4 in the metabolism of cholesterol and related bile acids (Table 3-2 and Figure 3-7, A-D). ATF4 was required for expression of several key genes involved in bile acid synthesis, which represents one pathway for disposing of free cholesterol in hepatocytes. Among these synthetic genes, *CYP7A1*, encoding cholesterol 7 alpha-hydroxylase, and *CYP27A1*, encoding sterol 27-hydroxylase, were significantly lowered in LsATF4-KO cells in both basal and ER stress conditions (Figure 3-7, A and B). Expression of *HNF4α*, a gene that enhances transcription of *CYP7A1* [108, 109] was also significantly reduced in LsATF4-KO livers. ATF4 is also required for full induction of *SOAT2*, which facilitates the conversion of free cholesterol to esterified cholesterol and was previously shown to be bound by ATF4 by ChiP-Seq (Figure 3-7, A and C) [54, 110, 111]. Free cholesterol can be damaging to cells through activation of JNK signaling and impairment of mitochondria membrane fluidity, and injury can be prevented by cholesterol esterification [73, 112, 113]. *nCEH1* was significantly reduced in response to ER stress independent of ATF4. Expression of genes responsible for exporting free cholesterol was also altered in the LsATF4-KO mice. *ABCG5* and *ABCG8* encode transporters that function on the enterocyte side of the hepatocyte, which export free cholesterol (Figure 3-7A) [114].

Expression of both genes were significantly reduced during ER stress, and loss of *ATF4* further lowered the amounts of *ABCG5* and *ABCG8* mRNAs during basal conditions (Figure 3-7D). *ABCA1* encodes a transporter of free cholesterol from hepatocytes to the plasma, and consistent with a previous report [115] *ABCA1* mRNA was reduced during ER stress. Deletion of *ATF4* decreased *ABCA1* expression basally (Figure 3-7D) and was found to be further reduced upon stress, which was found to be significant by two-way ANOVA of the interaction between treatment and the loss of *ATF4*. The key regulatory genes, *SREBP1* and *SREBP2*, were however, unaffected by the loss of *ATF4*. Together, these findings suggest that *ATF4* contributes to the expression of key genes involved in cholesterol metabolism and transport.

We next determined whether there are changes in free cholesterol levels upon loss of *ATF4* in response to ER stress. There were lowered levels of serum cholesterol basally in the Ls*ATF4*-KO mice compared to WT (Figure 3-7E), a finding consistent with that reported for Wb*ATF4*-KO [116]. Furthermore, cholesterol was lowered in both WT and Ls*ATF4*-KO mice after treatment with Tm (Figure 3-7E). While the Ls*ATF4*-KO mice trended towards lower total cholesterol during ER stress compared to WT, it did not reach statistical significance. We also measured the levels of free and total cholesterol in liver tissue (Figure 3-7F). Liver tissue from Ls*ATF4*-KO mice during stress showed significantly increased levels of free cholesterol, based on assays in the absence of esterase that represents free cholesterol.

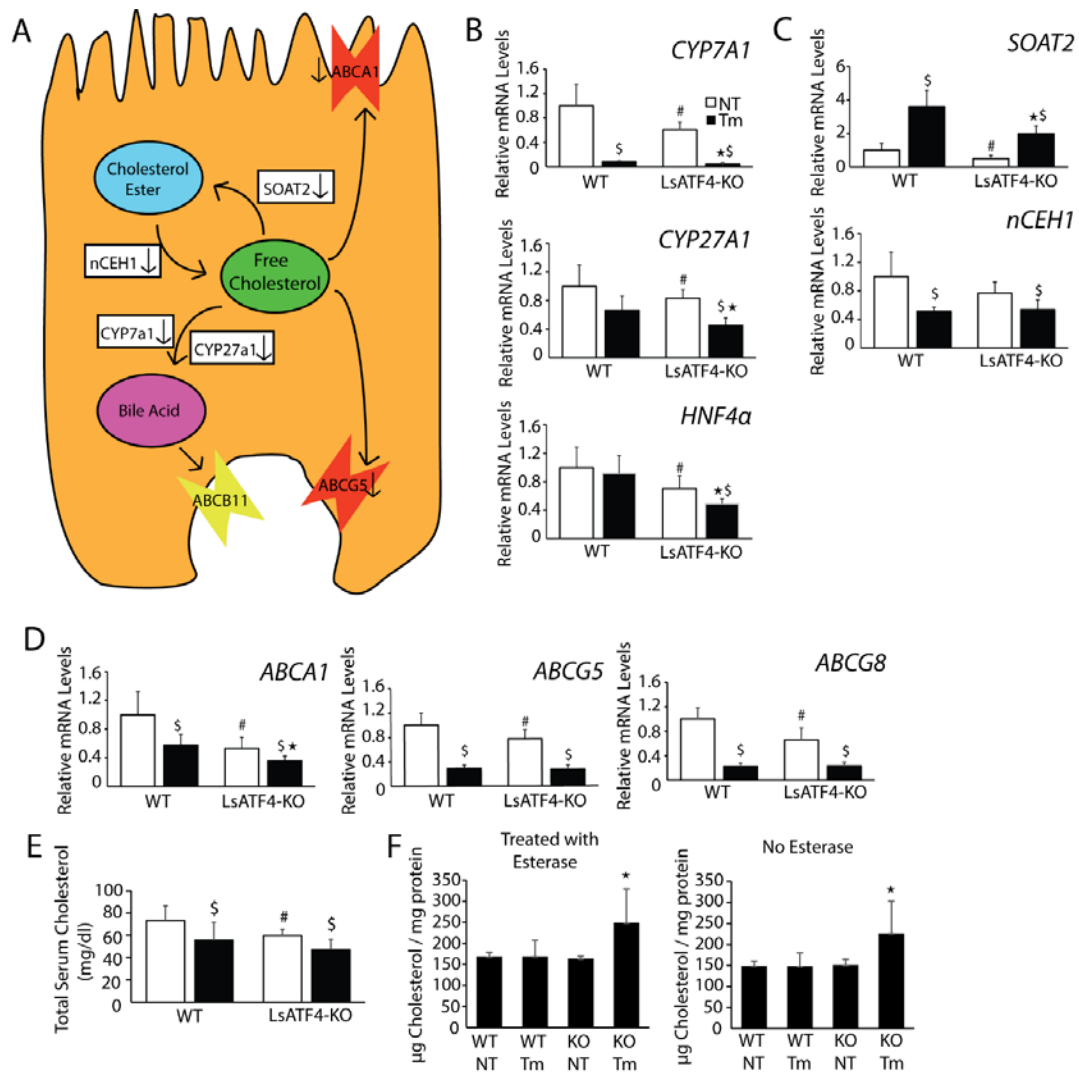


**Figure 3-7. Loss of *ATF4* leads to increased free cholesterol in liver.** (A)

Illustration of *ATF4*-targeted gene functions in hepatocyte cholesterol

metabolism. (B) WT and LsATF4-KO mice were injected IP with 1 mg/kg

tunicamycin (Tm) or vehicle (NT) for 6 hours. (B-D) Levels of the indicated

mRNAs were measured by qPCR and (E-F) cholesterol content by the Amplex

Red Cholesterol assay kit. (B-D) Genes involved in bile acid synthesis (*CYP7A1*,

*CYP27A1*, *HNF4a*), cholesterol esterification (*SOAT2*), or cholesterol export

(*ABCA1*, *ABCG5*, *ABCG8*) were significantly reduced due to loss of *ATF4*. (D-E)

WT and LsATF4-KO livers treated with Tm or vehicle were analyzed for total cholesterol content in the serum (E) and within the tissue (F). The “\*” indicates statistical significance ( $p < 0.05$ ) with respect to the ER treated tissues, “#”significance ( $p < 0.05$ ) among untreated tissues, and “\$” highlights significance between respective untreated ER stress tissues.



### 3.8 ATF4 basal expression is required for lipid metabolism

Given that Hepa1-6 shATF4 cells demonstrated lowered mitochondrial membrane potential (Figure 3-1F), we proposed that genes whose expression were reduced in the basal state adversely affected the mitochondria. Lipids play an important role in the structural integrity of the mitochondrial membrane, specifically the lipid cardiolipin, which is found almost exclusively in the mitochondria [117]. Cardiolipin is synthesized by the gene *CRLS1*, which was previously reported to be an ATF4-target gene by a genome-wide CHIP-Seq [54]. Deletions of this gene ortholog in yeast impair the electron transport chain and cause a decrease in mitochondrial membrane potential [118]. *CRLS1* is a member lipid metabolic process GO category identified by our PANTHER analysis of basal genes (Table 3-1) and demonstrated a significant reduction in expression in the RNA-seq. qRT-PCR of WT and LsATF4-KO mouse liver samples under basal conditions confirmed this reduction in expression, demonstrating a ~40% reduction in *CRLS1* mRNA expression (Figure 3-8A). This decrease was also seen at the CSRL1 protein level, where relative protein levels were reduced by ~50% (Figure 3-8B). These results suggest that ATF4 plays a direct role in the physiology of the mitochondria, and the energy production of the cell.

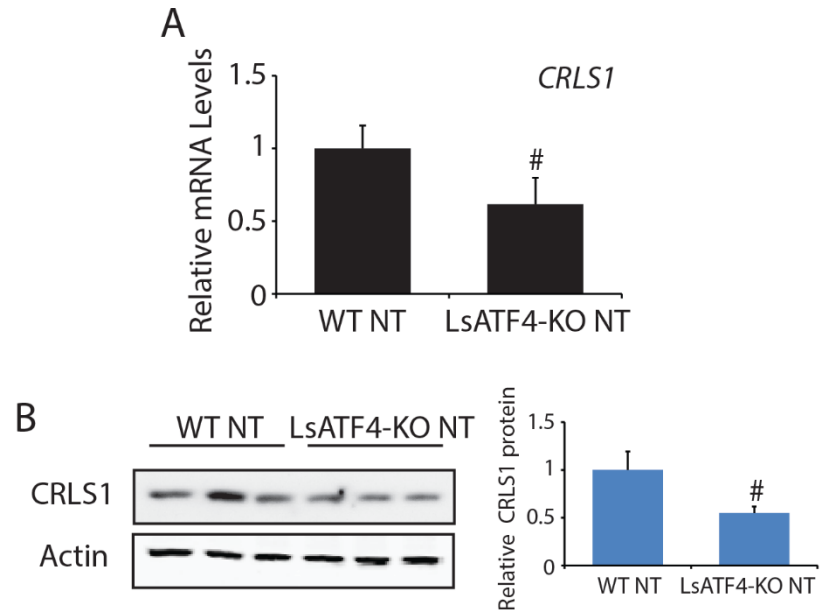


**Figure 3-8. Loss of ATF4 leads to reduced *CRLS1* expression.** (A) WT and LsATF4-KO mouse livers were collected and analyzed via qRT-PCR for *CRLS1* gene expression. (B) WT and LsATF4-KO mouse livers were collected and analyzed via immunoblot for expression of *CRLS1*. The image is representative of three separate immunoblots. Relative protein levels were assessed via ImageJ [90].

## CHAPTER 4. DISCUSSION

### 4.1 Similarities and differences in UPR signaling between cell culture models

The principal findings and models regarding ATF4 and its role in the ER stress response in earlier publications have been based largely on findings from MEF cell lines, and our results suggest that there can be variations between cell culture lines, and between cell culture and *in vivo*, though the possibility of 3D culture effects may also play a role [6, 46]. While certain characteristics were shared between cultured MEF, Hepa1-6 cells, and liver *in vivo*, there were also striking differences. Expression of ATF4 target genes *ASNS*, *FGF21*, and *CTH* were reduced upon loss of ATF4 regardless of the cell type studied (Figure 3-1, A and C). In contrast to MEF cells, ATF4 was not required for induced *CHOP* mRNA and protein in the Hepa1-6 cell line (Figure 3-1, C and D). *ATF6* expression was also unaffected by the loss of *ATF4* in liver, in contrast to data in MEF cells (Figure 3-1B) [25]. Whether this response is specific to the liver or an adaptive response to the loss of ATF4, is yet to be determined and warrants future investigation. ATF4 was previously suggested to play a role both in the transcription and transport of ATF6 in response to ER stress [25]. *ATF4*<sup>-/-</sup> MEFs fail to induce *ATF6* mRNA in response to stress, yet the results from the Hepa1-6 cell line would suggest that ATF4 does not play a major role in the transcription or transport of ATF6 (Figure 3-1B). These findings suggest that there could be another activating factor, or the basal levels of ATF6 are sufficient to elicit downstream responses upon activation.

*ATF4*<sup>-/-</sup> MEF cells have been previously associated with increased cell death, and an increase in oxidative stress in the basal condition [59]. Hepa1-6 cell lines that lacked *ATF4* expression showed a similar increase in cell death in response to prolonged ER stress (Figure 3-2D). The increase in cell death in these *ATF4*<sup>-/-</sup> cells is likely a consequence of lower expression of critical adaptive gene expression. It is important to note that there was continued *ATF4*-independent expression of the pro-apoptotic CHOP in the Hepa1-6 cells. This model of cell death would still vary from what is seen in MEF cell lines. MEF cells devoid of *ATF4* also lack expression of CHOP. Thus, cell death is attributed to the lack of *ATF4* pro-survival downstream targets, combined with lower CHOP. Differences in the mechanisms of cell death between the two cell lines are likely to depend on the presence or absence of oxidative stress. In MEF cells lacking *ATF4*, oxidative stress was present in the basal state as assessed by increased cell survival upon the addition of reducing compounds, such as  $\beta$ -mercaptoethanol [6], yet this oxidative stress was not present in the Hepa1-6 cell line model as measured by lipid peroxidation (Figure 3-1E). This dissimilarity could result from the physiological differences between a liver-derived Hepa1-6 cell line and the fibroblast-based MEF cells. The difference between the Hepa1-6 cell line, and Ls*ATF4*-KO mice may result from the media supplementation or represent a difference between culture and *in vivo*.

## 4.2 Role of crosstalk in the UPR

In the Hepa1-6 cell line, ATF6 was found to be central to *CHOP* expression during ER stress (Figure 3-2, A and B). In both *in vivo* and *in-vitro* models, PERK was shown to be required to elicit maximal expression of *ATF6* mRNA and activation of ATF6(N) [25]. These findings suggest a pathway for UPR activation that requires the PERK and ATF6 arms to elicit *CHOP* expression. This crosstalk is further expanded to include a role for ATF6 in the induced expression of *XBP1* mRNA (Figure 3-2A). These mechanisms of cross-talk imply that there are unique pathway functions in UPR activation rather than a system of redundancies. If ATF6 activation in response to ER stress were merely redundant with the ATF4 for activation of *CHOP*, loss of ATF4 would still diminish expression of *CHOP*. These unique activation pathways contributing to cross regulation of the UPR are also illustrated by the fact that ATF factors cannot replace each other, as illustrated by the finding that loss of ATF5 has no effect on *CHOP* expression, unlike the loss of ATF6 (Figure 3-2C).

In contrast to ER stress, there is some overlap in the pathways that activate ATF4 in response to cytosolic stresses that induce eIF2 $\alpha$ -P. For example, induction of *CHOP* expression was dependent upon both ATF4 and ATF6 during HF treatment that inhibits tRNA charging in the cytosol. This finding suggests that ATF4 is capable of driving *CHOP* expression within the liver, but this induction is dependent on the nature of the activating stress. It is noteworthy that there is a more modest activation of ATF6 during HF exposure compared with Tm (Figure 3-2 A and B, Figure 3-3 A and C). HF stress upregulates *ATF6* and *ATF4* mRNA but leads to the repression of *XBP1s* mRNA, supporting the

role of HF role as a cytosolic stress that does not appear to disrupt the ER. The lower level induced expression of ATF4 protein by HF also suggests that this stress activates the ISR to a lower extent than Tm treatment (Figure 3-3C). ATF6(N) protein expression was not detectable in the HF stress although *CHOP* mRNA levels would suggest that ATF6 still is a contributing activator. This was further supported by the ATF6 activity reporter, which showed significant induction upon HF treatment (Figure 3-3D).

ATF6 was previously shown to be a component of *CHOP* expression through an ESRE situated in its promoter [53]. The role of ATF6 has been overshadowed by the requirement in MEF culture cells on ATF4 binding to the amino acid response element (AARE) within the *CHOP* promoter [53, 119] and the idea that the three arms of the UPR operate independently. This switch from ATF4 to ATF6 -dependent *CHOP* expression may result in part from the timing of activation, with activation of ATF6 preceding that of ATF4 or the differential availability of the binding partners for ATF4 and ATF6. ATF6 is rapidly cleaved and activated upon ER stress, whereas ATF4 requires preferential translation and its induction occurs later in the UPR. The basic leucine zipper structure of ATF6 results in a preference for homodimerization, while ATF4 does not demonstrate a preference between homo and heterodimerization [120]. Thus, ATF4 not only requires upregulation of its own translation but can also be influenced by the nature of its binding partner. The timing may also explain why ATF5 does not play a role, unlike its other ATF family members ATF4 and ATF6. ATF5 is subject to preferential translational by a mechanism that is similar to

ATF4, and ATF5 has similar hetero- vs homo- dimerization preferences but requires ATF4 and CHOP for induction of its transcription [51, 120, 121]. The timing for induced ATF5 expression would therefore likely be too late for it to act as a primary driver of *CHOP* expression. These findings support the idea that the PERK/ATF6 crosstalk is a primary driver of *CHOP* expression within the liver during ER stress (Figure 3-3E). Furthermore, there is a network of feedforward transcriptional activation pathways that can rapidly amplify induction of the UPR transcriptome in response to an initiating ER insult.

#### **4.3 Role of ATF4 in the ER stress response *in vivo***

Our RNA-Seq analysis suggests an expanded role for ATF4-directed gene expression in liver under apparent basal conditions. 385 genes were significantly altered by the loss of *ATF4* in non-stressed conditions, which in fact exceeded those regulated during Tm treatment. The ATF4-target genes expressed during basal conditions are represented by metabolic processes of fatty acids and steroids, and cell adhesion (Table 3-1). ATF4 has previously been shown to promote metastasis in a tumor environment but is also required basally for the spread and progression of tumors [88].

Deletion of *ATF4* also significantly changed the expression of 352 genes among the set of 4717 genes altered during ER stress. The unexpected small subset of genes requiring ATF4 in the UPR compared to those involving PERK emphasizes that PERK can facilitate multiple transcriptional control networks beyond ATF4, including those of *ATF6* and *XBP1* [25]. Additionally, ATF4 and

CHOP ChIP-Seq analysis indicated that induced CHOP can play a direct role in the expression of genes that are also targeted by ATF4 [54]. Thus, PERK may be able to alleviate the loss of *ATF4* by exhibiting ATF4-independent expression of ATF6, ATF6-driven *CHOP* transcription, and CHOP upregulation of particular genes during ER stress.

Deletion of *ATF4* in liver further demonstrates its role in the prevention of oxidative stress independent of ER stress (Figure 3-5F). It is noted that there was no difference in MDA levels in cultured Hepa1-6 cells compared to those depleted for ATF4 (Figure 3-1E). Loss of ATF4 in the Hepa1-6 cells did lead to a striking reduction in mitochondrial membrane potential (Figure 3-1F), and diminished ROS production via oxidative phosphorylation may help explain the absence of observed oxidative stress in Hepa1-6 cells depleted for *ATF4*. Rapidly proliferating cells cultured in high media glucose concentration can proceed by aerobic glycolysis [122]. It was reported that ATF4 contributes to increased H<sub>2</sub>S sulfhydrylation of certain metabolic proteins during ER stress, altering their activity [123]. H<sub>2</sub>S sulfhydrylation occurs on several proteins within glycolysis and the TCA cycle, leading to an increase in glycolysis and a decrease in oxidative phosphorylation, which can be restored through CTH inhibition, which is in some manner mimicked by the loss of ATF4 [123].

#### **4.4 ATF4 and cholesterol metabolism**

Our biochemical and RNA-Seq analysis established the importance of ATF4 in the expression of genes important in cholesterol metabolism and



transport (Figure 3-7, B-D). Loss of *ATF4* led to decreased expression of *SOAT2*, a gene that was also identified as an *ATF4* and *CHOP* target by ChIP-Seq analyses (Table 3-1) [54], suggesting a lowered conversion of free cholesterol to cholesterol esters in the livers of *LsATF4-KO* mice (Figure 3-7, A and C). Free cholesterol would also be converted to bile acids at a reduced rate in the *ATF4*-deleted livers due to reduced expression of genes encoding *CYP7A1* and *CYP27A1* (Figure 3-7B). It would be expected that export of free cholesterol would be adversely affected in *LsATF4-KO* mice (Figure 3-7A). Previous studies suggested that ER stress results in ~50% reduction in *ABCA1* mRNA levels and decreased plasma cholesterol concentration [115, 116]. We determined that deletion of *ATF4* leads to a similar 50% reduction in *ABCA1* mRNA basally, which is further reduced by stress (Figure 3-7D). We also showed that ER stress triggered decreased sera cholesterol, which is further lowered both basally and during stress upon loss of *ATF4* (Figure 3-7E). Changes in gene expression and cholesterol levels may be a direct consequence of *ATF4* transcriptional regulation or indirect through downstream UPR effectors. Collectively these *ATF4*-directed changes in expression of genes involved in cholesterol metabolism and transport help explain the increased free cholesterol load within liver tissues of the *LsATF4-KO* mice (Figure 3-7F). Control of cholesterol metabolism via *ATF4* in the basal and ER stress state coincides with the protective role of *ATF4*. *ATF4* control of *SOAT2* expression allows cells to maintain appropriate levels of the potentially harmful free cholesterol, yet still allow for the conversion to bile acid [113]. Further investigation will be required

to delineate the direct roles of ATF4 in the metabolism of cholesterol. Currently, SOAT2 is the only known direct target of ATF4 in cholesterol metabolism, although the RNA-Seq analysis presented herein would suggest that there are others. The seemingly contradictory activation of SREBP and its transcriptional repression during ER stress could be suggested to allow for temporary alleviation of ER stress through ER expansion. The transcriptional repression of SREBP1 then would prevent further accumulation of lipids, as a result of *de novo* synthesis, alleviating a potential further stressor.

#### **4.5 Role of ATF4 in gene expression during the basal state**

Loss of ATF4 and the subsequent reduction in mitochondrial membrane reduction suggests a connection between ATF4 and the mitochondria in basal conditions. Cardiolipin has been associated with maintaining mitochondrial structure through a role in mitochondrial fusion/fission events and its association with members of the electron transport chain [118]. The reduction in cardiolipin synthetase mRNA and protein in *ATF4*-deleted livers (Figure 3-8, A and B) would suggest a more glycolytic means of energy production due to the role of cardiolipin in electron transport. The glycolytic pathway is preferred during periods of stress as ATF4 drives expression of *CTH* resulting in the sulfhydration of metabolic proteins, like pyruvate kinase 2, which results in increased activity promoting glycolysis [123]. The inhibition of *CTH*, however, prevents this increase in activity, and the loss of ATF4 reduces *CTH* expression and sulfhydration levels, and would be suggested to prevent the increase in pyruvate

kinase 2 activity typically seen during stress. These metabolic alterations could also explain why *ATF4*<sup>-/-</sup> MEF cells have a reduced growth rate [6]. Cells that are depleted for ATF4 show basal oxidative stress, along with sub-optimal oxidative phosphorylation due to the reduced cardiolipin levels, while being unable to optimally increase their glycolytic activity during periods of stress.

The role of ATF4 in metabolism, along with its differing functions in development among tissues suggest that a wide range of transcription factors can directly or indirectly interact with ATF4 to elicit its downstream effects on the target gene. This wide range of ATF4 effects, even in light of a reduced yet more specialized role within the UPR, suggest there is much more to learn about ATF4.

## REFERENCES

1. Walter, P. and D. Ron, *The unfolded protein response: from stress pathway to homeostatic regulation*. Science, 2011. **334**(6059): p. 1081-6.
2. Baird, T.D. and R.C. Wek, *Eukaryotic initiation factor 2 phosphorylation and translational control in metabolism*. Adv Nutr, 2012. **3**(3): p. 307-21.
3. Baird, T.D., et al., *Selective mRNA translation during eIF2 phosphorylation induces expression of IBTKalpha*. Mol Biol Cell, 2014. **25**(10): p. 1686-97.
4. Fu, S., S.M. Watkins, and G.S. Hotamisligil, *The role of endoplasmic reticulum in hepatic lipid homeostasis and stress signaling*. Cell Metab, 2012. **15**(5): p. 623-34.
5. Dey, S., et al., *Both transcriptional regulation and translational control of ATF4 are central to the integrated stress response*. J Biol Chem, 2010. **285**(43): p. 33165-74.
6. Harding, H.P., et al., *An integrated stress response regulates amino acid metabolism and resistance to oxidative stress*. Mol Cell, 2003. **11**: p. 619-33.
7. Vattem, K.M. and R.C. Wek, *Reinitiation involving upstream open reading frames regulates ATF4 mRNA translation in mammalian cells*. Proc Natl Acad Sci U.S.A., 2004. **101**: p. 11269-74.
8. Wek, R.C. and D.R. Cavener, *Translational Control and the Unfolded Protein Response*. Antioxid Redox Signal, 2007. **9**: p. 2357-71.

9. Hetz, C., et al., *The unfolded protein response: integrating stress signals through the stress sensor IRE1alpha*. *Physiol Rev*, 2011. **91**(4): p. 1219-43.
10. Calfon, M., et al., *IRE1 couples endoplasmic reticulum load to secretory capacity by processing of XBP-1 mRNA*. *Nature*, 2002. **415**: p. 92-96.
11. Lee, A.H., N.N. Iwakoshi, and L.H. Glimcher, *XBP-1 regulates a subset of endoplasmic reticulum resident chaperone genes in the unfolded protein response*. *Molecular and Cellular Biology*, 2003. **23**: p. 7448-7459.
12. Lee, K., et al., *IRE1-mediated unconventional mRNA splicing and S2P-mediated ATF6 cleavage merge to regulate XBP1 in signaling the unfolded protein response*. *Genes Dev*, 2002. **16**: p. 452-466.
13. Sidrauski, C. and P. Walter, *The transmembrane kinase Ire1p is a site-specific endonuclease that initiates mRNA splicing in the unfolded protein response*. *Cell*, 1997. **90**: p. 1031-1039.
14. Yamamoto, K., et al., *Transcriptional induction of mammalian ER quality control proteins is mediated by single or combined action of ATF6alpha and XBP1*. *Dev Cell*, 2007. **13**(3): p. 365-76.
15. Yoshida, H., et al., *XBP1 mRNA is induced by ATF6 and spliced by IRE1 in response to ER stress to produce a highly active transcription factor*. *Cell*, 2001. **107**: p. 881-891.
16. Tirasophon, W., A.A. Welihinda, and R.J. Kaufman, *A stress response pathway from the endoplasmic reticulum to the nucleus requires the*

- bifunctional protein kinase/endoribonuclease (Ire1p) in mammalian cells.*  
Genes and Development, 1998. **12**: p. 1812-1824.
17. Hollien, J. and J.S. Weissman, *Decay of endoplasmic reticulum-localized mRNAs during the unfolded protein response.* Science, 2006. **313**(5783): p. 104-107.
  18. Hollien, J., et al., *Regulated Ire1-dependent decay of messenger RNAs in mammalian cells.* J Cell Biol, 2009. **186**(3): p. 323-31.
  19. Bommiasamy, H., et al., *ATF6alpha induces XBP1-independent expansion of the endoplasmic reticulum.* J Cell Sci, 2009. **122**(Pt 10): p. 1626-36.
  20. Shen, J. and R. Prywes, *ER stress signaling by regulated proteolysis of ATF6.* Methods, 2005. **35**(4): p. 382-9.
  21. Wu, J., et al., *ATF6alpha optimizes long-term endoplasmic reticulum function to protect cells from chronic stress.* Dev Cell, 2007. **13**(3): p. 351-64.
  22. Schroder, M. and R.J. Kaufman, *Divergent roles of IRE1alpha and PERK in the unfolded protein response.* Curr Mol Med, 2006. **6**(1): p. 5-36.
  23. Lin, J.H., et al., *IRE1 signaling affects cell fate during the unfolded protein response.* Science, 2007. **318**(5852): p. 944-9.
  24. Lin, J.H., et al., *Divergent effects of PERK and IRE1 signaling on cell viability.* PLoS One, 2009. **4**(1): p. e4170.

25. Teske, B.F., et al., *The eIF2 kinase PERK and the integrated stress response facilitate activation of ATF6 during endoplasmic reticulum stress*. Mol Biol Cell, 2011. **22**: p. 4390-405.
26. Todd, D.J., A.H. Lee, and L.H. Glimcher, *The endoplasmic reticulum stress response in immunity and autoimmunity*. Nat Rev Immunol, 2008. **8**(9): p. 663-74.
27. Brewer, J.W., *Regulatory crosstalk within the mammalian unfolded protein response*. Cell Mol Life Sci, 2014. **71**(6): p. 1067-79.
28. Sonenberg, N. and A.G. Hinnebusch, *Regulation of translation initiation in eukaryotes: mechanisms and biological targets*. Cell, 2009. **136**(4): p. 731-45.
29. Algire, M.A., D. Maag, and J.R. Lorsch, *Pi release from eIF2, not GTP hydrolysis, is the step controlled by start-site selection during eukaryotic translation initiation*. Mol Cell, 2005. **20**(2): p. 251-62.
30. Lassot, I., et al., *ATF4 degradation relies on a phosphorylation-dependent interaction with the SCF(betaTrCP) ubiquitin ligase*. Molecular and Cellular Biology, 2001. **21**: p. 2192-2202.
31. Rutkowski, D.T., et al., *Adaptation to ER stress is mediated by differential stabilities of pro-survival and pro-apoptotic mRNAs and proteins*. PLoS Biol, 2006. **4**(11): p. e374.
32. Shen, J., et al., *ER stress regulation of ATF6 localization by dissociation of BiP/GRP78 binding and unmasking of Golgi localization signals*. Dev Cell, 2002. **3**(1): p. 99-111.

33. Shen, J., et al., *Stable binding of ATF6 to BiP in the endoplasmic reticulum stress response*. Mol Cell Biol, 2005. **25**(3): p. 921-32.
34. Wu, J. and R.J. Kaufman, *From acute ER stress to physiological roles of the Unfolded Protein Response*. Cell Death Differ, 2006. **13**(3): p. 374-84.
35. Chen, X., J. Shen, and R. Prywes, *The luminal domain of ATF6 senses endoplasmic reticulum (ER) stress and causes translocation of ATF6 from the ER to the Golgi*. J Biol Chem, 2002. **277**(15): p. 13045-52.
36. Ye, J., et al., *ER stress induces cleavage of membrane-bound ATF6 by the same proteases that process SREBPs*. Mol Cell, 2000. **6**(6): p. 1355-64.
37. Haze, K., et al., *Mammalian transcription factor ATF6 is synthesized as a transmembrane protein and activated by proteolysis in response to endoplasmic reticulum stress*. Molecular and Cellular Biology, 1999. **10**: p. 3787-3799.
38. Adachi, Y., et al., *ATF6 is a transcription factor specializing in the regulation of quality control proteins in the endoplasmic reticulum*. Cell Struct Funct, 2008. **33**(1): p. 75-89.
39. Xu, M., et al., *ATF6 Is Mutated in Early Onset Photoreceptor Degeneration With Macular Involvement*. Invest Ophthalmol Vis Sci, 2015. **56**(6): p. 3889-95.
40. Ansar, M., et al., *Mutation of ATF6 causes autosomal recessive achromatopsia*. Hum Genet, 2015. **134**(9): p. 941-50.



41. Liu, C.Y., M. Schroder, and R.J. Kaufman, *Ligand-independent dimerization activates the stress response kinases IRE1 and PERK in the lumen of the endoplasmic reticulum*. J Biol Chem, 2000. **275**(32): p. 24881-5.
42. Jurkin, J., et al., *The mammalian tRNA ligase complex mediates splicing of XBP1 mRNA and controls antibody secretion in plasma cells*. EMBO J, 2014. **33**(24): p. 2922-36.
43. Barbosa-Tessmann, I.P., et al., *Activation of the human asparagine synthetase gene by the amino acid response and the endoplasmic reticulum stress response pathways occurs by common genomic elements*. J Biol Chem, 2000. **275**(35): p. 26976-85.
44. Roybal, C.N., et al., *The oxidative stressor arsenite activates vascular endothelial growth factor mRNA transcription by an ATF4-dependent mechanism*. Journal of Biological Chemistry, 2005. **280**(21): p. 20331-9.
45. Kilberg, M.S., et al., *The transcription factor network associated with the amino acid response in mammalian cells*. Adv Nutr, 2012. **3**(3): p. 295-306.
46. Fusakio, M.E., et al., *Transcription factor ATF4 directs basal and select induced gene expression in the unfolded protein response and cholesterol metabolism in liver*. Mol Biol Cell, 2016.
47. Pan, Y.X., et al., *Activation of the ATF3 gene through a co-ordinated amino acid-sensing response programme that controls transcriptional*

*regulation of responsive genes following amino acid limitation.*

Biochemical Journal, 2007. **401**(1): p. 299-307.

48. Chen, H., et al., *Amino acid deprivation induces the transcription rate of the human asparagine synthetase gene through a timed program of expression and promoter binding of nutrient-responsive basic region/leucine zipper transcription factors as well as localized histone acetylation.* J Biol Chem, 2004. **279**: p. 50829-39.
49. Dickhout, J.G., et al., *Integrated stress response modulates cellular redox state via induction of cystathionine gamma-lyase: cross-talk between integrated stress response and thiol metabolism.* J Biol Chem, 2012. **287**(10): p. 7603-14.
50. Su, N. and M.S. Kilberg, *C/EBP homology protein (CHOP) interacts with activating transcription factor 4 (ATF4) and negatively regulates the stress-dependent induction of the asparagine synthetase gene.* J Biol Chem, 2008. **283**(50): p. 35106-17.
51. Teske, B.F., et al., *CHOP induces activating transcription factor 5 (ATF5) to trigger apoptosis in response to perturbations in protein homeostasis.* Mol Biol Cell, 2013. **24**(15): p. 2477-90.
52. Wang, X.Z., et al., *Signals from the stress endoplasmic reticulum induce C/EBP homologous protein (CHOP/GADD153).* Molecular and Cellular Biology, 1996. **16**: p. 4273-4280.

53. Ma, Y., et al., *Two distinct stress signaling pathways converge upon the CHOP promoter during the mammalian unfolded protein response*. J Mol Biol, 2002. **318**: p. 1351-65.
54. Han, J., et al., *ER-stress-induced transcriptional regulation increases protein synthesis leading to cell death*. Nat Cell Biol, 2013. **15**(5): p. 481-90.
55. Marciniak, S.J., et al., *CHOP induces death by promoting protein synthesis and oxidation in the stressed endoplasmic reticulum*. Genes Dev, 2004. **18**(24): p. 3066-77.
56. Novoa, I., et al., *Feedback inhibition of the unfolded protein response by GADD34-mediated dephosphorylation of eIF2alpha*. J Cell Biol, 2001. **153**: p. 1011-22.
57. Connor, J.H., et al., *Growth arrest and DNA damage-inducible protein GADD34 assembles a novel signaling complex containing protein phosphatase 1 and inhibitor 1*. Mol Cell Biol, 2001. **21**: p. 6841-50.
58. Brush, M.H., D.C. Weiser, and S. Shenolikar, *Growth arrest and DNA damage-inducible protein GADD34 targets protein phosphatase 1 alpha to the endoplasmic reticulum and promotes dephosphorylation of the alpha subunit of eukaryotic translation factor 2*. Molecular and Cellular Biology, 2003. **23**: p. 1292-1303.
59. Harding, H.P., et al., *Ppp1r15 gene knockout reveals an essential role for translation initiation factor 2 alpha (eIF2alpha) dephosphorylation in*

- mammalian development*. Proc Natl Acad Sci U S A, 2009. **106**(6): p. 1832-7.
60. Kim, E., *Mechanisms of amino acid sensing in mTOR signaling pathway*. Nutr Res Pract, 2009. **3**(1): p. 64-71.
61. Kilberg, M.S., et al., *Nutritional control of gene expression: how mammalian cells respond to amino acid limitation*. Annual Review of Nutrition, 2005. **25**: p. 59-85.
62. Zoncu, R., A. Efeyan, and D.M. Sabatini, *mTOR: from growth signal integration to cancer, diabetes and ageing*. Nat Rev Mol Cell Biol, 2011. **12**(1): p. 21-35.
63. Bar-Peled, L. and D.M. Sabatini, *Regulation of mTORC1 by amino acids*. Trends Cell Biol, 2014. **24**(7): p. 400-6.
64. Ye, J., et al., *GCN2 sustains mTORC1 suppression upon amino acid deprivation by inducing Sestrin2*. Genes Dev, 2015. **29**(22): p. 2331-6.
65. Buel, G.R. and J. Blenis, *CELL SIGNALING. Seeing mTORC1 specificity*. Science, 2016. **351**(6268): p. 25-6.
66. Katiyar, S., et al., *REDD1, an inhibitor of mTOR signalling, is regulated by the CUL4A-DDB1 ubiquitin ligase*. EMBO Rep, 2009. **10**(8): p. 866-72.
67. Chaudhari, N., et al., *A molecular web: endoplasmic reticulum stress, inflammation, and oxidative stress*. Front Cell Neurosci, 2014. **8**: p. 213.
68. Finkel, T. and N.J. Holbrook, *Oxidants, oxidative stress and the biology of ageing*. Nature, 2000. **408**(6809): p. 239-247.

69. Zhou, H. and R. Liu, *ER stress and hepatic lipid metabolism*. Front Genet, 2014. **5**: p. 112.
70. Rutkowski, D.T., et al., *UPR pathways combine to prevent hepatic steatosis caused by ER stress-mediated suppression of transcriptional master regulators*. Dev Cell, 2008. **15**(6): p. 829-40.
71. Osborne, T.F. and P.J. Espenshade, *Evolutionary conservation and adaptation in the mechanism that regulates SREBP action: what a long, strange tRIP it's been*. Genes Dev, 2009. **23**(22): p. 2578-91.
72. Dietschy, J.M., S.D. Turley, and D.K. Spady, *Role of liver in the maintenance of cholesterol and low density lipoprotein homeostasis in different animal species, including humans*. J Lipid Res, 1993. **34**(10): p. 1637-59.
73. Arguello, G., et al., *Recent insights on the role of cholesterol in non-alcoholic fatty liver disease*. Biochim Biophys Acta, 2015. **1852**(9): p. 1765-78.
74. Chaveroux, C., et al., *In vivo imaging of the spatiotemporal activity of the eIF2alpha-ATF4 signaling pathway: Insights into stress and related disorders*. Sci Signal, 2015. **8**(374): p. rs5.
75. Fischer, C., et al., *Activating transcription factor 4 is required for the differentiation of the lamina propria layer of the vas deferens*. Biol Reprod, 2004. **70**(2): p. 371-8.

76. Yang, X., et al., *ATF4 is a substrate of RSK2 and an essential regulator of osteoblast biology; implication for Coffin-Lowry Syndrome*. Cell, 2004. **117**(3): p. 387-98.
77. Tanaka, T., et al., *Targeted disruption of ATF4 discloses its essential role in the formation of eye lens fibres*. Genes Cells, 1998. **3**(12): p. 801-10.
78. Masuoka, H.C. and T.M. Townes, *Targeted disruption of the activating transcription factor 4 gene results in severe fetal anemia in mice*. Blood, 2002. **99**(3): p. 736-745.
79. Ebert, S.M., et al., *The transcription factor ATF4 promotes skeletal myofiber atrophy during fasting*. Mol Endocrinol, 2010. **24**(4): p. 790-9.
80. Ebert, S.M., et al., *Identification and Small Molecule Inhibition of an Activating Transcription Factor 4 (ATF4)-dependent Pathway to Age-related Skeletal Muscle Weakness and Atrophy*. J Biol Chem, 2015. **290**(42): p. 25497-511.
81. Yu, S., et al., *General transcription factor IIA-gamma increases osteoblast-specific osteocalcin gene expression via activating transcription factor 4 and runt-related transcription factor 2*. J Biol Chem, 2008. **283**(9): p. 5542-53.
82. Cao, H., et al., *Activating transcription factor 4 regulates osteoclast differentiation in mice*. J Clin Invest, 2010. **120**(8): p. 2755-66.
83. Fox, D.K., et al., *p53 and ATF4 mediate distinct and additive pathways to skeletal muscle atrophy during limb immobilization*. Am J Physiol Endocrinol Metab, 2014. **307**(3): p. E245-61.

84. Dey, S., et al., *Transcriptional repression of ATF4 gene by CCAAT/enhancer-binding protein beta (C/EBPbeta) differentially regulates integrated stress response*. J Biol Chem, 2012. **287**(26): p. 21936-49.
85. Gardner, L.B., *Hypoxic inhibition of nonsense-mediated RNA decay regulates gene expression and the integrated stress response*. Mol Cell Biol, 2008. **28**(11): p. 3729-41.
86. Senée, V., et al., *Wolcott-Rallison syndrome: clinical, genetic, and functional study of EIF2AK3 mutations, and suggestion of genetic heterogeneity*. Diabetes, 2004. **53**: p. 1876-83.
87. Suzuki, T., N. Osumi, and Y. Wakamatsu, *Stabilization of ATF4 protein is required for the regulation of epithelial-mesenchymal transition of the avian neural crest*. Dev Biol, 2010. **344**(2): p. 658-68.
88. Dey, S., et al., *ATF4-dependent induction of heme oxygenase 1 prevents anoikis and promotes metastasis*. J Clin Invest, 2015. **(in press)**  
**doi:10.1172/JCI78031**.
89. Willy, J.A., et al., *CHOP links endoplasmic reticulum stress to NF-kB activation in the pathogenesis of nonalcoholic steatophepatitis*. Manuscript submitted, 2015.
90. Schneider, C.A., W.S. Rasband, and K.W. Eliceiri, *NIH Image to ImageJ: 25 years of image analysis*. Nat Methods, 2012. **9**(7): p. 671-5.
91. Ebert, S.M., et al., *Stress-induced skeletal muscle Gadd45a expression reprograms myonuclei and causes muscle atrophy*. J Biol Chem, 2012. **287**(33): p. 27290-301.

92. Wang, Y., et al., *Activation of ATF6 and an ATF6 DNA binding site by the endoplasmic reticulum stress response*. Journal of Biological Chemistry, 2000. **275**: p. 27013-27020.
93. Liu, D., et al., *Nuclear import of proinflammatory transcription factors is required for massive liver apoptosis induced by bacterial lipopolysaccharide*. J Biol Chem, 2004. **279**(46): p. 48434-42.
94. Woo, Y.C., et al., *Fibroblast growth factor 21 as an emerging metabolic regulator: clinical perspectives*. Clin Endocrinol (Oxf), 2013. **78**(4): p. 489-96.
95. De Sousa-Coelho, A.L., P.F. Marrero, and D. Haro, *Activating transcription factor 4-dependent induction of FGF21 during amino acid deprivation*. Biochem J, 2012. **443**(1): p. 165-71.
96. Ayala, A., M.F. Munoz, and S. Arguelles, *Lipid peroxidation: production, metabolism, and signaling mechanisms of malondialdehyde and 4-hydroxy-2-nonenal*. Oxid Med Cell Longev, 2014. **2014**: p. 360438.
97. Baumeister, P., et al., *Endoplasmic reticulum stress induction of the Grp78/BiP promoter: activating mechanisms mediated by YY1 and its interactive chromatin modifiers*. Mol Cell Biol, 2005. **25**(11): p. 4529-40.
98. Marciniak, S.J. and D. Ron, *Endoplasmic reticulum stress signaling in disease*. Physiol Rev, 2006. **86**(4): p. 1133-49.
99. Puthalakath, H., et al., *ER stress triggers apoptosis by activating BH3-only protein Bim*. Cell, 2007. **129**(7): p. 1337-49.



100. Osowski, C.M. and F. Urano, *The binary switch that controls the life and death decisions of ER stressed beta cells*. *Curr Opin Cell Biol*, 2011. **23**(2): p. 207-15.
101. Peng, W., et al., *Surgical stress resistance induced by single amino acid deprivation requires Gcn2 in mice*. *Sci Transl Med*, 2012. **4**(118): p. 118ra11.
102. Sundrud, M.S., et al., *Halofuginone inhibits TH17 cell differentiation by activating the amino acid starvation response*. *Science*, 2009. **324**(5932): p. 1334-8.
103. Trapnell, C., L. Pachter, and S.L. Salzberg, *TopHat: discovering splice junctions with RNA-Seq*. *Bioinformatics*, 2009. **25**(9): p. 1105-11.
104. Trapnell, C., et al., *Differential gene and transcript expression analysis of RNA-seq experiments with TopHat and Cufflinks*. *Nat Protoc*, 2012. **7**(3): p. 562-78.
105. Trapnell, C., et al., *Transcript assembly and quantification by RNA-Seq reveals unannotated transcripts and isoform switching during cell differentiation*. *Nat Biotechnol*, 2010. **28**(5): p. 511-5.
106. Mi, H. and P. Thomas, *PANTHER pathway: an ontology-based pathway database coupled with data analysis tools*. *Methods Mol Biol*, 2009. **563**: p. 123-40.
107. Mi, H., A. Muruganujan, and P.D. Thomas, *PANTHER in 2013: modeling the evolution of gene function, and other gene attributes, in the context of*

- phylogenetic trees*. Nucleic Acids Res, 2013. **41**(Database issue): p. D377-86.
108. De Fabiani, E., et al., *The negative effects of bile acids and tumor necrosis factor-alpha on the transcription of cholesterol 7alpha-hydroxylase gene (CYP7A1) converge to hepatic nuclear factor-4: a novel mechanism of feedback regulation of bile acid synthesis mediated by nuclear receptors*. J Biol Chem, 2001. **276**(33): p. 30708-16.
109. Kir, S., et al., *Nuclear receptors HNF4alpha and LRH-1 cooperate in regulating Cyp7a1 in vivo*. J Biol Chem, 2012. **287**(49): p. 41334-41.
110. Cases, S., et al., *ACAT-2, a second mammalian acyl-CoA:cholesterol acyltransferase. Its cloning, expression, and characterization*. J Biol Chem, 1998. **273**(41): p. 26755-64.
111. Zhao, B., J. Song, and S. Ghosh, *Hepatic overexpression of cholesteryl ester hydrolase enhances cholesterol elimination and in vivo reverse cholesterol transport*. J Lipid Res, 2008. **49**(10): p. 2212-7.
112. Kellner-Weibel, G., et al., *Effects of intracellular free cholesterol accumulation on macrophage viability: a model for foam cell death*. Arterioscler Thromb Vasc Biol, 1998. **18**(3): p. 423-31.
113. Feng, B., et al., *The endoplasmic reticulum is the site of cholesterol-induced cytotoxicity in macrophages*. Nat Cell Biol, 2003. **5**(9): p. 781-92.
114. Lu, K., et al., *Two genes that map to the STSL locus cause sitosterolemia: genomic structure and spectrum of mutations involving sterolin-1 and*

- sterolin-2, encoded by ABCG5 and ABCG8, respectively.* Am J Hum Genet, 2001. **69**(2): p. 278-90.
115. Rohrl, C., et al., *Endoplasmic reticulum stress impairs cholesterol efflux and synthesis in hepatic cells.* J Lipid Res, 2014. **55**(1): p. 94-103.
116. Xiao, G., et al., *ATF4 protein deficiency protects against high fructose-induced hypertriglyceridemia in mice.* J Biol Chem, 2013. **288**(35): p. 25350-61.
117. Tocchi, A., et al., *Mitochondrial dysfunction in cardiac aging.* Biochim Biophys Acta, 2015. **1847**(11): p. 1424-33.
118. de Paepe, R., S.D. Lemaire, and A. Danon, *Cardiolipin at the heart of stress response across kingdoms.* Plant Signal Behav, 2014. **9**.
119. Bruhat, A., et al., *Differences in the molecular mechanisms involved in the transcriptional activation of CHOP and asparagine synthetase in response to amino acid deprivation or activation of the unfolded protein response.* Journal of Biological Chemistry, 2002. **277**: p. 48107-48114.
120. Vinson, C., et al., *Classification of human B-ZIP proteins based on dimerization properties.* Mol Cell Biol, 2002. **22**(18): p. 6321-35.
121. Zhou, D., et al., *Phosphorylation of eIF2 directs ATF5 translational control in response to diverse stress conditions.* J Biol Chem, 2008. **283**(11): p. 7064-73.
122. Vander Heiden, M.G., L.C. Cantley, and C.B. Thompson, *Understanding the Warburg effect: the metabolic requirements of cell proliferation.* Science, 2009. **324**(5930): p. 1029-33.

123. Gao, X.H., et al., *Quantitative H<sub>2</sub>S-mediated protein sulfhydration reveals metabolic reprogramming during the integrated stress response*. *Elife*, 2015. 4.

## CURRICULUM VITAE

Michael Edward Fusakio

### EDUCATION:

**Indiana University, IBMG Program Ph.D.** (2011-2016)

Ph.D. in Biochemistry and Molecular Biology

Minors in Diabetes and Bioinformatics

Relevant Coursework: Diabetes & Obesity, Programming for Life

Sciences, Next Generation Sequencing

**Coursera Online Courses** (2015-Present)

John Hopkins Data Science Specialization: The Data Scientist's  
Toolbox, R Programming, Getting and Cleaning Data, Exploratory  
Data Analysis, and Reproducible Research

John Hopkins Genomic Data Science Specialization: Introduction to  
Genomic Tech, Genomic Data Science with Galaxy, Python for  
Genomic Data Science, Algorithms for DNA Sequencing, Command  
Line Tools for Genomic Data Science, Bioconductor for Genomic Data  
Science, Statistics for Genomic Data Science

**DePauw University** (2005-2009)

BA in Biochemistry

Minor in Philosophy

Awards and Honors: Phi Lambda Upsilon (National Honorary  
Chemistry Society), Cum Laude GPA: 3.52/4.0

RESEARCH EXPERIENCE:

**Indiana University School of Medicine** (2011-2016)

**Graduate Researcher** – Biochemistry Department with Dr. Ronald Wek

- Investigate the complex signaling and signal crosstalk involved in the Unfolded Protein Response and the role this signaling plays in liver physiology and development of Non-alcoholic Steatohepatitis and Diabetes.
- Characterized signaling pathway response during endoplasmic reticulum stress in mouse and cell culture models.
- Develop through certified self-taught online and in-class courses the necessary skills to prepare, analyze, interpret, and present RNA-Seq and Microarray data examining the effect of gene alterations upon the Unfolded Protein Response.

**Cincinnati Children's Hospital** (2009-2011)

**Research Assistant II** – Immunobiology Department with Dr. Jochen

Mattner

- Analyzed inflammatory and autoimmune response of the liver focusing on Primary Biliary Cirrhosis.
- Acquired and analyzed complex histological and molecular data from

mouse and cell culture models.

- Maintained 25 breeding lines of mice, through the use of time and project management skills to assign specific mouse lines as needed for my experiments.

#### TEACHING EXPERIENCE:

##### **IU School of Medicine**

###### **Biochemistry Student Representative to the Faculty** (2014-2015)

- Served as the representative of the student body of the Biochemistry department in faculty meetings concerning new departmental policy.

###### **Medical Student Tutor** (2014)

- Selected to tutor medical student in Biochemistry.

###### **Graduate Student Teaching Assistant, Biomedical Science I** (2013)

- Assigned to tutor incoming graduate students, managed review sessions for a class of 25 graduate students.

##### **DePauw University**

###### **Undergraduate Teaching Assistant, Animal Physiology** (2008)

- Lead student labs in coordination with the professor, also lead class discussion. Taught section of 20 students.

#### TEAMWORK EXPERIENCE:

##### **Indiana University School of Medicine**

###### **Travel Grant Review Board** (2014-2015)

- Consulted as part of seven member board to evaluate winners of program travel grant.
- Ranked 25 applications per cycle and participated in committee meetings to review and finalize travel grant award winners.

#### PUBLICATIONS:

1. **Fusakio ME**, Willy JA, Wang Y, Mirek ET, Al-Baghdadi RJT, Adams CM, Anthony TG, and Wek RC. "Transcription Factor ATF4 directs basal and select induced gene expression in the unfolded protein response and cholesterol metabolism in liver." Mol Biol Cell. 2016 Epub March 9.
2. Gabriel Josiah Wilson, Brittany A Lennox, Pengxiang She, Emily T Mirek, Rana J T Al-Baghdadi, **Michael E Fusakio**, Joseph Dixon, Gregory C Henderson, Ronald C Wek, Tracy G Anthony. (2014) GCN2 is required to increase fibroblast growth factor 21 and maintain hepatic triglyceride homeostasis during asparaginase treatment. Am J Physiol Endocrinol Metab. 2015 Feb 15;308(4):e283-93.
3. Baird TD, Palam LR, **Fusakio ME**, Willy JA, Davis CM, McClintick JN, Anthony TG, Wek RC. (2014). Selective mRNA translation during eIF2 phosphorylation induces expression of IBTK $\alpha$ . Mol Biol Cell. 25(10): 1686-97.



4. Brian F. Teske, **Michael E. Fusakio**, Donghui Zhou, Jixiu Shan, Jeanette N. McClintick, Michael S. Kilberg, and Ronald C. Wek. (2013) CHOP Induces Activating Transcription Factor 5 (ATF5) to Trigger Apoptosis in Response to Perturbations in Protein Homeostasis. *Mol Biol Cell*. 2013 Aug;24(15): 2477-90
  
5. **Fusakio ME**, Mohammed JP, Laumonier Y, Hoebe K, Köhl J, Mattner J. (2011) C5a regulates NKT and NK cell function in sepsis. *J Immunol*. 187(11): 5805-5812.
  
6. Mohammed JP, **Fusakio ME**, Rainbow DB, Moule C, Fraser HI, Clark J, Todd JA, Peterson LB, Savage PB, Wills-Karp M, Ridgway WM, Wicker LS, Mattner J. (2011) Identification of Cd101 as a susceptibility gene for *Novosphingobium aromaticivorans*-induced liver autoimmunity. *J Immunol*. 187(1): 337-349
  
7. Rainbow DB, Moule C, Fraser HI, Clark J, Howlett SK, Burren O, Christensen M, Moody V, Steward CA, Mohammed JP, **Fusakio ME**, Masteller EL, Finger EB, Houchins JP, Naf D, Koentgen F, Ridgway WM, Todd JA, Bluestone JA, Peterson LB, Mattner J, Wicker LS. (2011) Evidence that Cd101 is an autoimmune diabetes gene in nonobese diabetic mice. *J Immunol*. 187(1):325-336

#### MEETINGS:

- **Michael E. Fusakio**, Brian F. Teske, and Ronald C. Wek. 2012. "CHOP induces the expression of the transcription factor ATF5 to trigger apoptosis." Cold Spring Harbor Meeting for Translational Control. Cold Spring Harbor, New York.
- **Michael E. Fusakio**, Brian F. Teske, and Ronald C. Wek. 2014. "Perk is required to activate multiple arms of the unfolded protein response." FASEB Science Research Conference on Nutrient Sensing and Metabolic Signaling. Big Sky, MT.

#### ORAL PRESENTATIONS:

- "Development of NASH through the exacerbation of the UPR" Indiana Fatty Liver Research Group. 2012. Indianapolis, IN.

#### AWARDS:

- T32 Training Grant Diabetes and Obesity. 2013-2016. T32DK064466
- FASEB Travel Award. 2014. FASEB Science Research Conference on Nutrient Sensing and Metabolic Signaling. Big Sky, MT